

特邀综述

# 多功能超疏水表面的制造和应用研究现状

闫德峰, 刘子艾, 潘维浩, 赵丹阳, 宋金龙

(大连理工大学, 辽宁 大连 116024)

**摘 要:** 荷叶表面是自然界中典型的超疏水表面, 具有“出淤泥而不染”的特性, 近年来, 荷叶表面的超疏水现象引起了科研人员的广泛关注。普通表面经构建微米级粗糙结构和低表面能修饰后, 可获得超疏水表面。将水滴置于超疏水表面上, 水滴与超疏水表面间存在一层空气垫, 空气垫可有效减小水滴与表面的接触面积, 使水滴无法浸入表面微观结构中, 而被“支撑”在超疏水表面上, 因此超疏水表面对水表现出优异的排斥性。这种特殊性能使超疏水表面在诸多领域都有极高的应用前景和 market 价值。本文对超疏水基础原理进行了梳理, 并对近期超疏水领域的研究成果进行了综述。首先介绍了超疏水表面的经典润湿理论, 包括 Young 模型、Wenzel 模型和 Cassie-Baxter 模型。然后归纳了诸多超疏水表面的制备方法及其优缺点, 包括激光刻蚀法、化学沉积法、化学刻蚀法、电化学沉积法、电化学刻蚀法、热氧化法、喷涂法等。在分析不同制造方法的基础上, 进一步讨论了超疏水表面在自清洁、防雾、抗结冰、耐腐蚀、液体无损转移、油水分离、摩擦发电、芯片实验室、液滴传感器等领域的应用。最后, 指出超疏水表面从实验室研究走向生产应用过程中所面临的问题, 并对超疏水表面的未来发展进行展望。

**关键词:** 超疏水表面; 微纳米粗糙结构; 低表面能; 制造方法; 多功能应用

**中图分类号:** O647 **文献标识码:** A **文章编号:** 1001-3660(2021)05-0001-19

**DOI:** 10.16490/j.cnki.issn.1001-3660.2021.05.001

## Research Status on the Fabrication and Application of Multifunctional Superhydrophobic Surfaces

YAN De-feng, LIU Zi-ai, PAN Wei-hao, ZHAO Dan-yang, SONG Jin-long

(Dalian University of Technology, Dalian 116024, China)

**ABSTRACT:** The upper surface of the lotus leaf is a typical superhydrophobic surface in nature world, which has the special characteristic of self-cleaning. In recent years, the superhydrophobic phenomenon on the upper surface of the lotus leaf has aroused much attention of researchers. The superhydrophobic surfaces can be obtained by constructing the micro/nano rough

收稿日期: 2020-10-31; 修订日期: 2021-03-24

Received: 2020-10-31; Revised: 2021-03-24

基金项目: 国家自然科学基金 (51605078); 中国科协青年人才托举工程 (2017QNRC001); 航空科学基金 (2017ZE63012); 大连市科技之星项目 (2018RQ01)

Fund: Supported by the National Natural Science Foundation of China (51605078), the Young Elite Scientists Sponsorship Program by CAST (2017QNRC001), the Aviation Science Fund (2017ZE63012), Dalian Youth Science and Technology Star (2018RQ01)

作者简介: 闫德峰 (1994—), 男, 博士研究生, 主要研究方向为非传统加工技术与装备。

Biography: YAN De-feng (1994—), Male, Doctor candidate, Research focus: non-traditional machining technology and equipment.

通讯作者: 宋金龙 (1987—), 男, 博士, 副研究员, 主要研究方向为非传统加工技术与装备。邮箱: songjinlong@dlut.edu.cn

Corresponding author: SONG Jin-long (1987—), Male, Doctor, Associate professor, Research focus: non-traditional machining technology and equipment. E-mail: songjinlong@dlut.edu.cn

引文格式: 闫德峰, 刘子艾, 潘维浩, 等. 多功能超疏水表面的制造和应用研究现状[J]. 表面技术, 2021, 50(5): 1-19.

YAN De-feng, LIU Zi-ai, PAN Wei-hao, et al. Research status on the fabrication and application of multifunctional superhydrophobic surfaces [J]. Surface technology, 2021, 50(5): 1-19.

structures and modification of low surface energy. Researchers found that when a water droplet is placed on the superhydrophobic surfaces, the physical barrier of air cushion is formed between a water droplet and the superhydrophobic surfaces. The air cushion can effectively reduce the contact area of water droplets with the superhydrophobic surfaces, so that the water droplet cannot be immersed in the micro/nano rough structures of superhydrophobic surfaces and is supported on the superhydrophobic surfaces, therefore the superhydrophobic surface shows special properties of waterproof. In the past few decades, researchers found that the superhydrophobic surfaces had practical application value and far-reaching prospect. This paper reviews the basic principles of superhydrophobic surfaces and the recent research achievements in the superhydrophobic fields. First of all, the classical wetting models of superhydrophobic surfaces are introduced, including the Young model, the Wenzel model and the Cassie-Baxter model. Then, the basic methods of preparing superhydrophobic surfaces are summarized, such as laser etching, chemical deposition, chemical etching, electrochemical deposition, electrochemical etching, thermal oxidation, ect. In addition, the applications of superhydrophobic surfaces, such as self-cleaning, anti-fogging, anti-icing, corrosion resistance, lossless transport of liquid, oil-water separation, triboelectric nanogenerator, lab-on-a-chip, and droplet sensor is discussed based on the analysis of different manufacturing methods. Finally, the problems needed to be resolved from the laboratory research to the industrial application of the superhydrophobic surfaces are pointed out, and the urgently demanded research focus and promising development trend of this field are prospected.

**KEY WORDS:** superhydrophobic surfaces; micro/nano rough structures; low surface energy; fabrication methods; multifunctional applications

液体在固体表面的铺展能力称为该固体的润湿性，润湿性由固体表面微观结构和化学组成共同决定，常用接触角来衡量<sup>[1]</sup>。接触角是固-液-气三相交点处的液-气界面切线与固-液两相边界线的夹角，如图 1 所示。接触角在  $0^\circ \sim 90^\circ$  时，为亲液表面；接触角在  $90^\circ \sim 180^\circ$  时，为疏液表面。亲液表面中，接触角小于  $10^\circ$  时，为超亲液表面；疏液表面中，接触角大于  $150^\circ$  时，为超疏液表面<sup>[2]</sup>。德国科学家 Barthlott<sup>[3]</sup>通过扫描电子显微镜（SEM）观察荷叶上表面时，发现荷叶上表面的超疏水性是由其表面的微米级乳突结构（图 2a）和表面蜡状物共同引起的。江雷等<sup>[4]</sup>进一

步研究发现，该乳突结构表面还存在纳米晶体结构（图 2b），这些微纳米结构和表面蜡状物质使荷叶上表面具有超疏水性能。

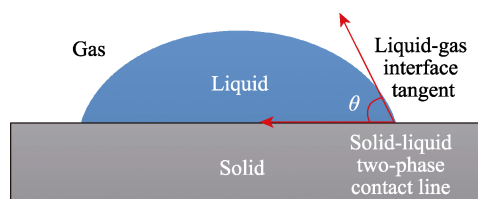
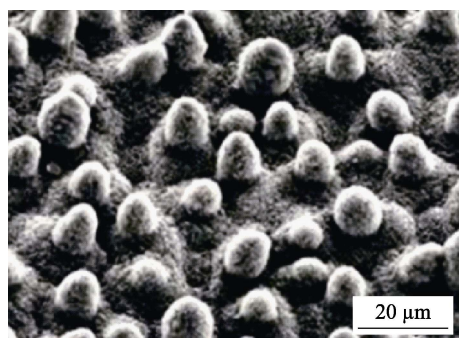
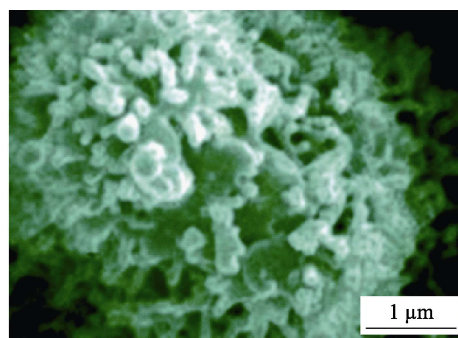


图 1 接触角示意图<sup>[2]</sup>

Fig.1 Schematic diagram of contact angle<sup>[2]</sup>



a 微米级乳突结构<sup>[3]</sup>



b 纳米晶体结构<sup>[4]</sup>

图 2 荷叶上表面微观形貌

Fig.2 Micro-topography of the upper surface of lotus leaf: a) micro-sized mastoid structures<sup>[3]</sup>; b) nano-sized crystal structures<sup>[4]</sup>

## 1 经典润湿性理论

### 1.1 Young 模型

Young<sup>[5]</sup>认为液体在理想的光滑固体表面上时，

其接触角只与固-气、固-液、液-气界面的表面张力有关（图 3a），而理想固体表面的接触角称为本征接触角  $\theta_Y$ ，本征接触角满足 Young 方程：

$$\cos \theta_Y = (\gamma_{SG} - \gamma_{SL}) / \gamma_{LG} \quad (1)$$

式中： $\gamma_{SG}$  为固-气界面的表面张力， $\gamma_{SL}$  为固-液

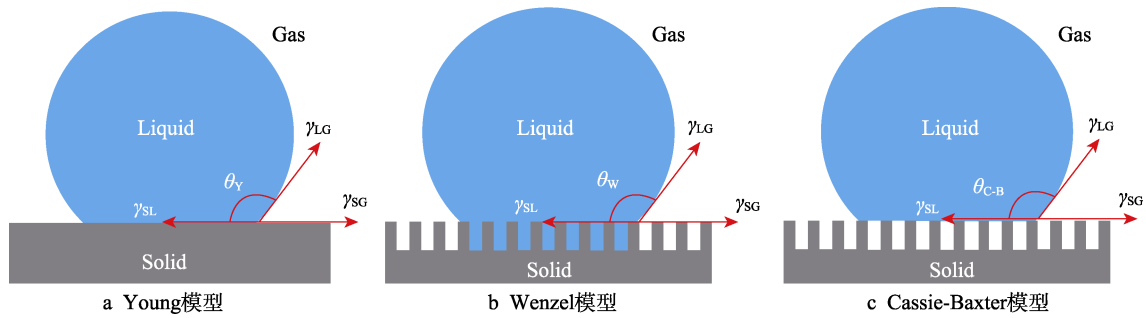


图 3 表面润湿性经典理论

Fig.3 Classical models of surface wetting: a) Young model; b) Wenzel model; c) Cassie-Baxter model

界面的表面张力,  $\gamma_{LG}$  为液-气界面的表面张力。该公式表明, 当  $\gamma_{LG}$  为定值时, 本征接触角  $\theta_Y$  随着  $\gamma_{SG}-\gamma_{SL}$  值的减小而增大。

## 1.2 Wenzel 模型

由于实际固体表面并非是理想的光滑表面, 其表面通常具有微观粗糙结构 (图 3b)。因此 Wenzel<sup>[6]</sup>对 Young 模型进行修正并提出了 Wenzel 模型, 此时液滴接触角方程为:

$$\cos \theta_w = r(\gamma_{SG} - \gamma_{SL}) / \gamma_{LG} = r \cos \theta_Y \quad (2)$$

式中:  $\theta_w$  为 Wenzel 模型下的表观接触角;  $r$  为粗糙度因子, 其值为固-液两相实际接触面积与表观接触面积之比。由于固体表面具有微观粗糙结构, 实际接触面积大于表观接触面积, 因此  $r > 1$ 。根据式(2)可得, 当  $\theta_Y < 90^\circ$  时, 表面粗糙度增加, 可使亲液表面更亲液; 当  $\theta_Y > 90^\circ$  时, 表面粗糙度增加, 可使疏液表面更疏液。

## 1.3 Cassie-Baxter 模型

Cassie 和 Baxter<sup>[7]</sup>发现天然超疏水表面具有微观粗糙结构, 但液滴并不是完全充满表面的粗糙结构, 因此提出了一种新的润湿模型, 即 Cassie-Baxter 模型 (图 3c)。该模型中, 液滴底部并未与固体的粗糙结构底部接触, 而是被粗糙结构内部的空气垫隔开, 液滴底部同时与固体、气体接触, 形成由固-液-气三相组成的复合接触面。在 Cassie-Baxter 润湿模型下, 液滴的接触角方程如下:

$$\cos \theta_{C-B} = f_1 \cos \theta_Y - f_2 \quad (3)$$

式中:  $\theta_{C-B}$  为 Cassie-Baxter 润湿模型下的表观接触角;  $f_1$ 、 $f_2$  分别为固-液两相界面和液-气两相界面在复合接触面上所占比例。由式(3)可得, 当  $\theta_Y > 90^\circ$  时 (即疏液表面),  $\theta_{C-B}$  随  $f_1$  减小而增大。因此, 在 Cassie-Baxter 润湿模型下, 通过减少固-液接触面积 (即增加固体表面粗糙结构), 可增大接触角  $\theta_{C-B}$ 。

## 2 超疏水表面的常见制备方法

受自然界中超疏水表面的启发, 近几十年来, 研究人员以金属<sup>[8-10]</sup>、玻璃<sup>[11-13]</sup>、织物<sup>[14-16]</sup>、水泥<sup>[17-19]</sup>

等材料为基底, 通过不同加工手段及制造方法制备出多种超疏水表面<sup>[20-22]</sup>。根据润湿性相关理论可知, 超疏水表面是由其表面的微纳米粗糙结构及表面的化学成分共同引起的<sup>[23-25]</sup>。目前, 研究人员开发了诸多制备超疏水表面的加工方法, 根据加工原理的不同, 可分为激光刻蚀法<sup>[26-28]</sup>、化学沉积法<sup>[29-31]</sup>、化学刻蚀法<sup>[32-34]</sup>、电化学沉积法<sup>[35-37]</sup>、电化学刻蚀法<sup>[38-40]</sup>、热氧化法<sup>[41-43]</sup>、喷涂法<sup>[44-46]</sup>等。

### 2.1 激光刻蚀法

激光刻蚀法是利用光热效应在样品表面加工出微纳米级粗糙结构的方法。Liu 等<sup>[26]</sup>通过纳秒激光加工器刻蚀铝表面, 激光蚀刻过程中, 铝表面的熔化和固化产生了直径 1~5  $\mu\text{m}$  的球形颗粒 (图 4a), 经硬脂酸修饰后, 可获得超疏水铝表面, 如图 4b 所示。Zhang 等<sup>[27]</sup>通过纳秒激光加工器在镁合金表面刻蚀出鹿角状微观粗糙结构 (图 4c), 该表面经十三氟辛基三乙氧基硅烷修饰后, 获得水接触角约为  $161^\circ$  的超疏水表面。Yong 等<sup>[28]</sup>利用飞秒激光加工器在聚二甲基硅氧烷 (PDMS) 表面刻蚀出由几十至几百纳米的纳米结构组成的不规则微观粗糙结构 (图 4d), 由于 PDMS 自身为低表面能材料, 无需进行低表面能修饰即可获得接触角约为  $162^\circ$  的超疏水 PDMS 表面。激光刻蚀法具有加工精度高、加工过程简单的特点, 可高效率地构建复杂的微纳米级粗糙结构, 但激光刻蚀法通常需要依赖特殊的加工设备, 价格比较昂贵。

### 2.2 化学沉积法

化学沉积法是利用溶液中的离子与金属基底发生化学反应, 生成物在基底表面沉积, 从而形成微观粗糙结构的方法。Huang 等<sup>[29]</sup>将不锈钢片浸泡在硫酸镍和过硫酸钾的混合溶液中, 在不锈钢片表面沉积出直径几百纳米的球状结构 (图 5a), 经全氟辛酸修饰后, 获得接触角约为  $158^\circ$  的超疏水不锈钢片表面。Jia 等<sup>[30]</sup>将镁合金片浸泡在硝酸银溶液中, 使镁合金表面沉积出如图 5b 所示的微纳米级粗糙结构, 该粗糙结构由直径 2~3  $\mu\text{m}$  的微球结构组成, 微球结构表面不规则地排列着厚度约为 100 nm 的薄片, 该表面经硬脂酸修饰后, 可获得接触角约为  $153^\circ$  的超疏水镁合金



表面。Zhu 等<sup>[31]</sup>将铜片浸泡在硝酸银溶液中,使铜片表面沉积出珊瑚状的粗糙结构,如图 5c 所示。经全氟辛酸修饰后,获得了接触角约为  $163^\circ$  的超疏水铜片

表面。化学沉积法具有制备工艺简单、反应条件可控的特点,但化学沉积法一般只能置换活性较弱的金属,而且这些金属大多价格昂贵,制备成本较高。

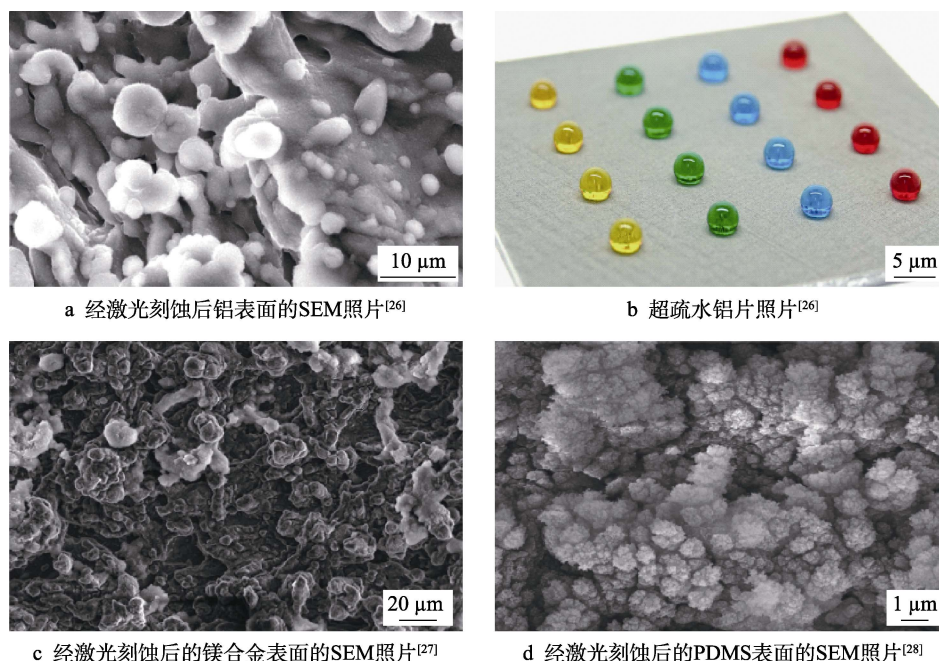


图 4 利用激光刻蚀法制造超疏水表面

Fig.4 Fabrication of superhydrophobic surfaces by laser etching: a) SEM image of the aluminum surface after laser etching<sup>[26]</sup>; b) image of the superhydrophobic aluminum plate<sup>[26]</sup>; c) SEM image of the magnesium alloy surface after laser etching<sup>[27]</sup>; d) SEM image of the PDMS surface after laser etching<sup>[28]</sup>

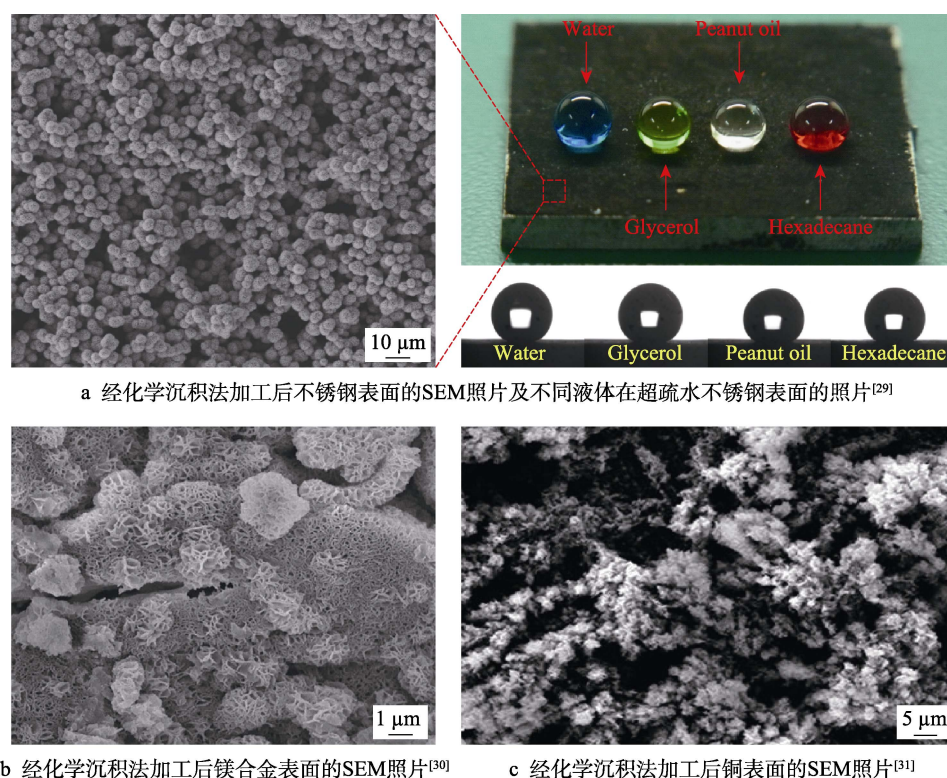


图 5 利用化学沉积法制造超疏水表面

Fig.5 Fabrication of superhydrophobic surfaces by chemical deposition: a) SEM image of the stainless steel surface after chemical deposition and images of the different droplets on the surface of superhydrophobic stainless steel<sup>[29]</sup>; b) SEM image of the magnesium alloy surface after chemical deposition<sup>[30]</sup>; c) SEM image of the copper surface after chemical deposition<sup>[31]</sup>



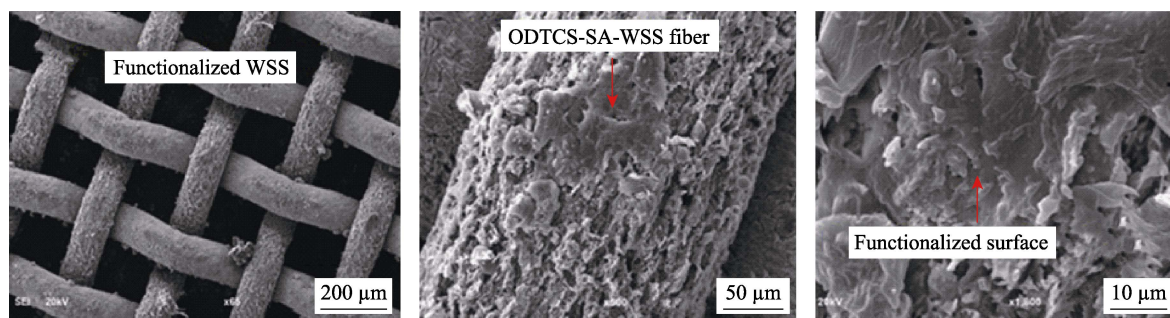
## 2.3 化学刻蚀法

化学刻蚀法是利用金属基底与刻蚀液发生化学反应，在基底表面形成微观粗糙结构的方法。Saleh 等<sup>[32]</sup>利用硫酸溶液在不锈钢网的网丝表面刻蚀出如图 6a 所示的微纳米级粗糙结构，该不锈钢网经十八烷基三氯硅烷修饰后，得到的接触角约为  $166^\circ$ ，超疏水性较好。Xiao 等<sup>[33]</sup>利用盐酸在铝片表面刻蚀出台阶状的粗糙结构，如图 6b 所示。经 3-巯丙基三乙氧基硅烷修饰后，获得超疏水性，水滴在其表面的接触角约为  $163^\circ$ 。Liu 等<sup>[34]</sup>利用氨水溶液对铜片表面进行化学刻蚀，生成了柳絮状的粗糙结构，如图 6c 所示，

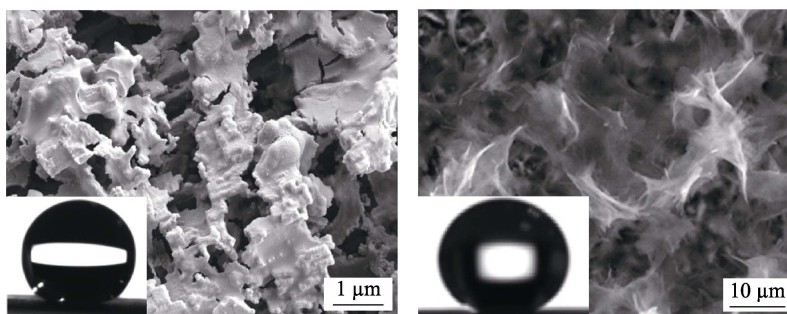
经硬脂酸修饰后获得接触角约为  $157^\circ$  的超疏水表面。化学刻蚀法具有制作工艺简单、成本低廉的特点，但刻蚀液通常为强酸/强碱等溶液，对环境 and 实验人员有一定危害。

## 2.4 电化学沉积法

电化学沉积法是将基底表面置于阴极使其发生电化学反应，在基底表面沉积生成具有微纳米级粗糙结构的方法。Tan 等<sup>[35]</sup>利用电化学沉积法在铁片表面沉积出大量的微米级叠层晶体，形成微观粗糙结构，经硬脂酸修饰后，获得接触角约为  $154^\circ$  的超疏水表面，如图 7a 所示。Liu 等<sup>[36]</sup>将镁合金片放入含有六



a 经化学刻蚀后不锈钢网的SEM照片<sup>[32]</sup>

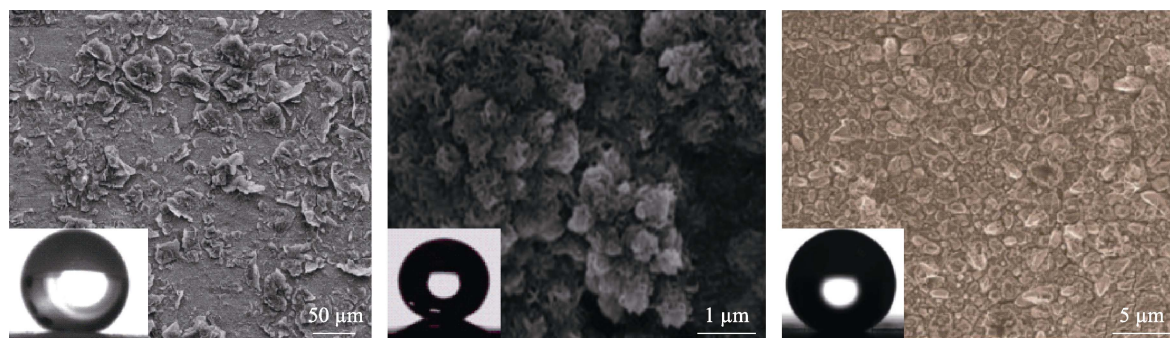


b 经化学刻蚀后铝表面的SEM照片<sup>[33]</sup>

c 经化学刻蚀后铜表面的SEM照片<sup>[34]</sup>

图 6 利用化学刻蚀法制造超疏水表面

Fig.6 Fabrication of superhydrophobic surfaces by chemical etching: (a) SEM images of the stainless steel mesh after chemical etching<sup>[32]</sup>; (b) SEM image of the aluminum surface after chemical etching<sup>[33]</sup>; (c) SEM image of the copper surface after chemical etching<sup>[34]</sup>



a 经电化学沉积后铁表面的SEM照片<sup>[35]</sup>

b 经电化学沉积后镁合金表面的SEM照片<sup>[36]</sup>

c 经电化学沉积后铜表面的SEM照片<sup>[37]</sup>

图 7 利用电化学沉积法制造超疏水表面

Fig.7 Fabrication of superhydrophobic surfaces by electrochemical deposition: a) SEM image of the steel surface after electrochemical deposition<sup>[35]</sup>; b) SEM image of the magnesium alloy surface after electrochemical deposition<sup>[36]</sup>; c) SEM image of the copper surface after electrochemical deposition<sup>[37]</sup>

水合硝酸铈和肉豆蔻酸的乙醇混合溶液中进行电化学沉积, 沉积出珊瑚状的粗糙结构, 由于肉豆蔻酸为低表面能物质, 因此通过一步电化学沉积即可获得接触角约为  $160^\circ$  的超疏水镁合金片表面, 如图 7b 所示。Su 等<sup>[37]</sup>采用电化学沉积法在铜表面沉积镍纳米粒子, 形成了松锥状的团簇粗糙结构, 经 1H,1H,2H,2H-全氟癸基三乙氧基硅烷修饰后, 获得接触角达到  $162^\circ$  的超疏水铜表面, 如图 7c 所示。电化学沉积法具有成本低廉、制备过程简单的特点, 但通过电化学沉积法制备的超疏水表面易磨损, 机械强度较差。

## 2.5 电化学刻蚀法

电化学刻蚀法是将基底表面置于阳极使其发生电化学反应, 刻蚀基底表面并在表面生成微纳米级粗糙结构的方法。Liu 等<sup>[38]</sup>以硝酸钠为刻蚀液, 通过电

化学刻蚀法在 30Cr2Ni2WVA 航空钢表面加工出高强度钝化膜, 该钝化膜具有珊瑚状的微观结构, 经十三氟辛基三乙氧基硅烷修饰后获得超疏水性, 水滴在其表面的接触角约为  $165^\circ$ , 滚动角约为  $5^\circ$ , 如图 8a 所示。Lu 等<sup>[39]</sup>以高氯酸为刻蚀液, 利用电化学刻蚀法在铝表面构建了珊瑚状的微纳米级粗糙结构, 经 1H,1H,2H,2H-全氟癸基三乙氧基硅烷修饰后获得超疏水性, 水滴在其表面接触角约为  $167^\circ$ , 如图 8b 所示。Li 等<sup>[40]</sup>以氯化钠和硝酸钠的混合溶液为刻蚀液在镁合金表面构建微粗糙结构, 经十三氟辛基三乙氧基硅烷修饰后获得接触角约为  $162^\circ$  的超疏水镁合金表面。电化学刻蚀法具有制备过程简单、成本低廉的特点, 但电化学刻蚀法只能加工导电材料, 难以加工活泼性较弱的金属。

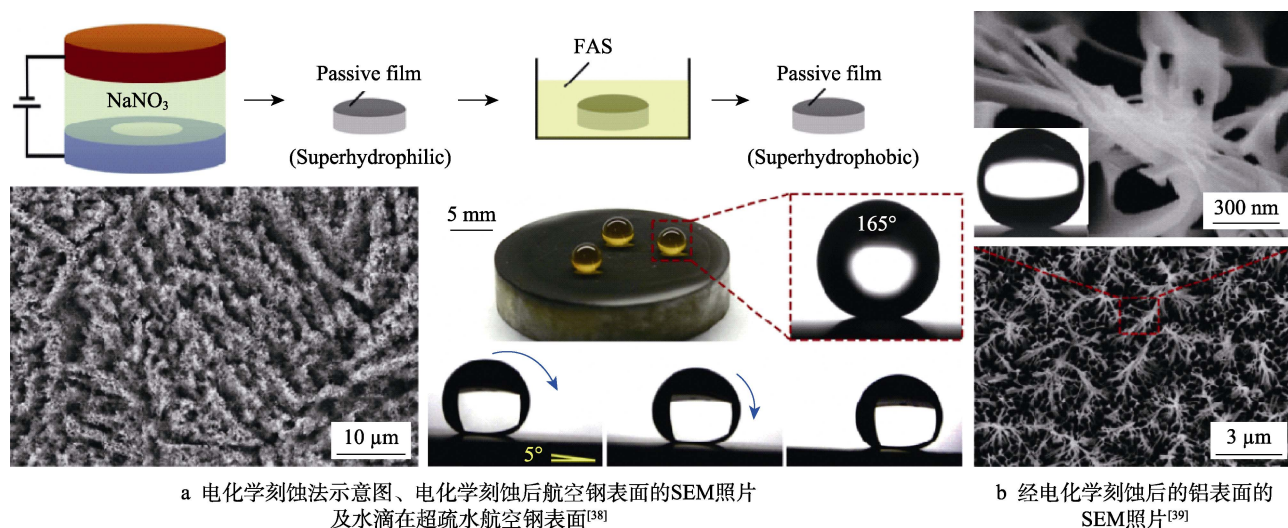


图 8 利用电化学刻蚀法制造超疏水表面

Fig.8 Fabrication of superhydrophobic surfaces by electrochemical etching: a) schematic diagram of the electrochemical etching processes, SEM image of the aeronautical steel surface after electrochemical etching and images of the water droplet on the superhydrophobic aeronautical steel surface<sup>[38]</sup>; b) SEM images of the aluminum surface after electrochemical etching<sup>[39]</sup>

## 2.6 热氧化法

热氧化法是将基底置于高温条件下, 使基底表面发生氧化反应并在表面生成微纳米级粗糙结构的方法。LV 等<sup>[41]</sup>先将铝片浸入硫酸铜溶液使其表面生成一层铜单质, 随后在  $550^\circ\text{C}$  下发生氧化反应, 生成氧化铜粗糙结构, 最后经硬脂酸修饰获得接触角约为  $157^\circ$  的超疏水表面, 如图 9a 所示。Cao 等<sup>[42]</sup>利用热氧化法在  $180^\circ\text{C}$  下使铜与硫发生化学反应, 铜片表面生成颗粒状的硫化铜和硫化亚铜粗糙结构, 经十三氟辛基三乙氧基硅烷修饰后获得接触角约为  $153^\circ$  的超疏水铜表面, 如图 9b 所示。Kang 等<sup>[43]</sup>将钛片置于  $1000^\circ\text{C}$  下与氧气发生氧化反应, 生成了台阶状的二氧化钛粗糙结构, 台阶状的粗糙结构表面分布着几百纳米大小的颗粒结构, 该表面经正十八烷基三氯硅烷修饰后获得接触角约为  $166^\circ$  的超疏水性, 如图 9c 所

示。热氧化法具有应用范围广、成本低廉的特点, 但在制备过程中通常需要高温处理, 存在一定安全隐患。

## 2.7 喷涂法

喷涂法是先将喷涂的微纳米颗粒提前进行低表面能修饰, 然后将修饰后的微纳米颗粒喷涂到基底表面, 进而使基底表面获得超疏水性的方法。Deng 等<sup>[44]</sup>将被月桂酸修饰的氢氧化铜悬浊液喷涂到铜网的网丝表面, 涂覆的网丝表面被氢氧化铜悬浊液覆盖, 形成了许多突起和凹陷, 烘干后获得接触角约为  $158^\circ$  的超疏水铜网, 如图 10a 所示。Wang 等<sup>[45]</sup>在铝合金片表面先喷涂一层烃类树脂作为粘接剂, 随后喷涂经二氯二甲基硅烷修饰的二氧化钛 ( $\text{TiO}_2$ ) 纳米粒子, 最终获得涂层微观结构如图 10b 所示的超疏水铝合金表面。Lu 等<sup>[46]</sup>利用喷涂法将经十三氟辛基三乙氧基硅烷修饰的  $\text{TiO}_2$  颗粒通过粘接剂固定在各种基底



上,喷涂后的基底均具有超疏水性,图 10c 为玻璃基底上超疏水  $\text{TiO}_2$  涂层的微观形貌。喷涂法经济简便、

可用于复杂形貌的基底表面,但通常涂层与基底结合力差,超疏水表面耐久度低。

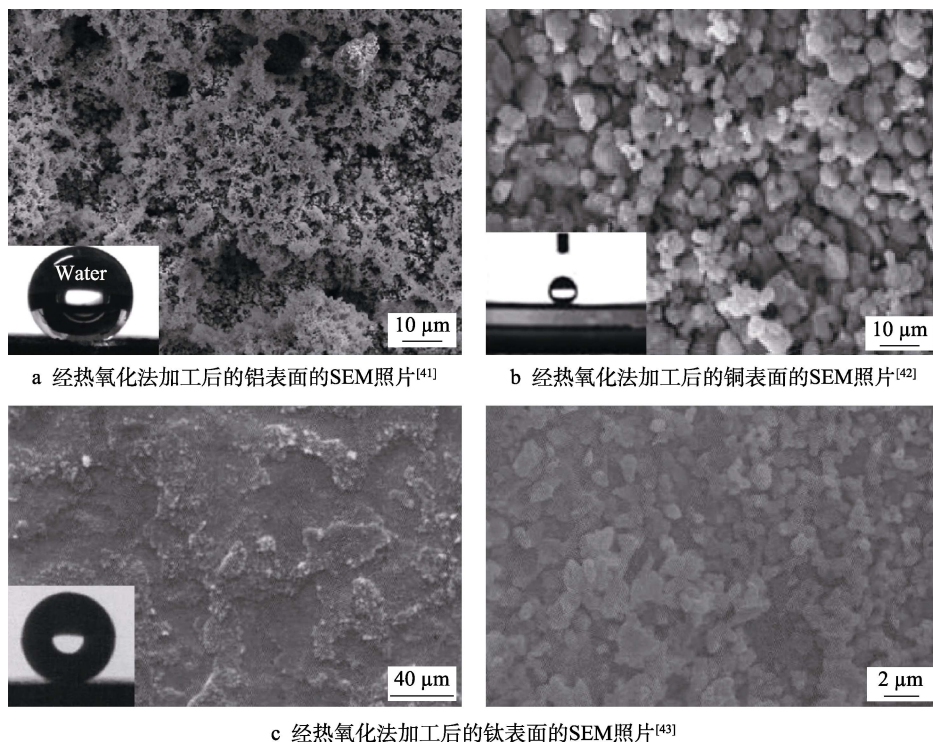


图 9 利用热氧化法制造超疏水表面

Fig.9 Fabrication of superhydrophobic surfaces by thermal oxidation: a) SEM image of the aluminum surface after thermal oxidation<sup>[41]</sup>, b) SEM image of the copper surface after thermal oxidation<sup>[42]</sup>, c) SEM images of the titanium surface after thermal oxidation<sup>[43]</sup>

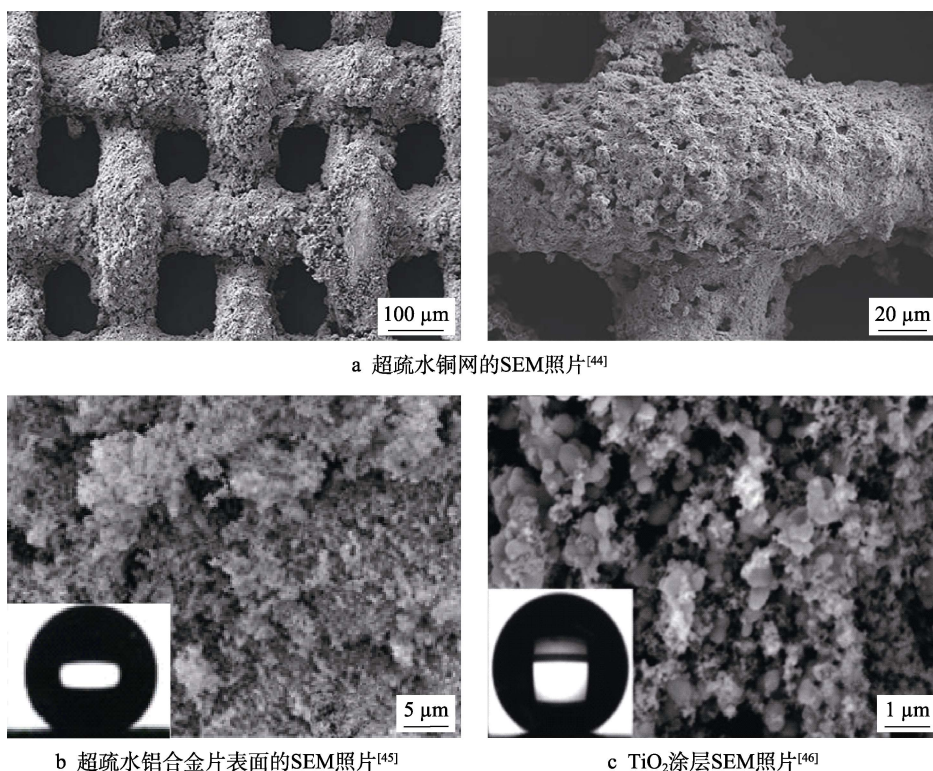


图 10 利用喷涂法制造超疏水表面

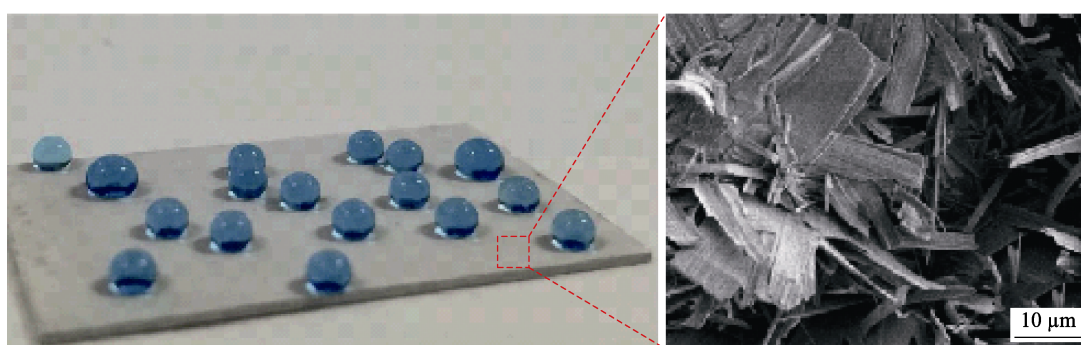
Fig.10 Fabrication of superhydrophobic surfaces by spraying: a) SEM images of the superhydrophobic copper mesh<sup>[44]</sup>, b) SEM image of the superhydrophobic aluminum alloy surface<sup>[45]</sup>, c) SEM image of the  $\text{TiO}_2$  coating<sup>[46]</sup>



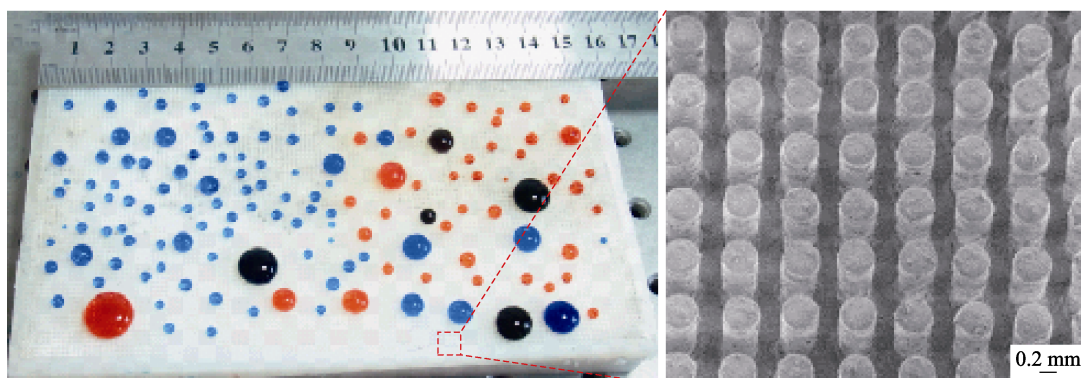
## 2.8 其他方法

常用的制备超疏水表面的方法还包括:水热法<sup>[47-49]</sup>、模板法<sup>[50-52]</sup>、光刻法<sup>[53-55]</sup>等。Zhang 等<sup>[49]</sup>利用水热法将 5083 铝合金片和全氟辛酸水溶液置入高压反应釜中,在 120 °C 下加热 4 h 以上,获得了超疏水铝合金片,该表面微观形貌呈现为片状微结构,水滴在表面的接触角约为 166°,如图 11a 所示。传统的制造方法一般较难大面积制备具有超疏水性能的表面,针对此问题, Song 等<sup>[50]</sup>利用模板法大面积制造出具有超疏水性能的柱状阵列表面,该小组先通过激光加工出具有阵列通孔的铝模板,随后将固化剂与环氧树脂搅拌均匀后,浇注在铝模板上,固化后取模,并喷涂 Never

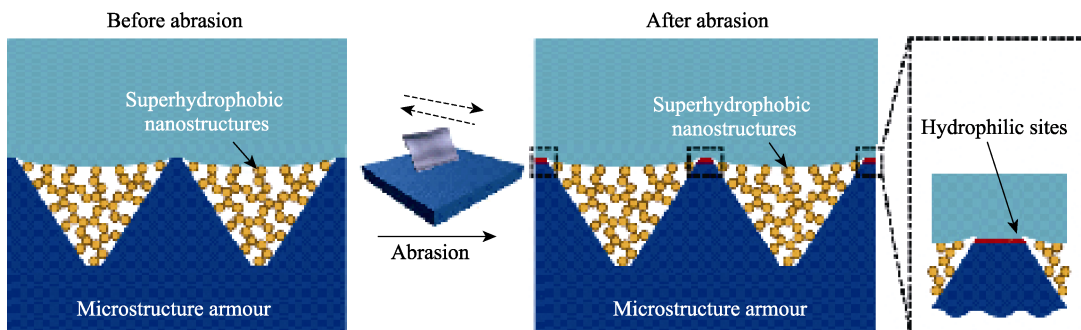
Wet 进行低表面能修饰,最终获得具有超疏水性能的柱状阵列表面,如图 11b 所示。Deng 等<sup>[54]</sup>首先利用光刻法在硅片表面加工出具有金字塔形结构的“铠甲”,随后将纳米级尺寸的蜡烛烟灰填充入金字塔形结构的凹坑内,最后经低表面能修饰后,获得超疏水表面。该方法通过在不同尺度上构造表面来实现超疏水性,其中纳米尺寸的蜡烛烟灰提供了疏水性,而微米级的结构则提供了耐用性。微米结构是一个相互连接的金字塔形框架,框架内为具有超疏水性能的纳米结构,该框架起到了“铠甲”的作用,如图 11c 所示,即使受到砂纸和刀片的破坏,所得超疏水表面的超疏水性仍然得以保持。



a 水滴在超疏水铝合金片表面的照片及超疏水铝合金片表面的SEM照片<sup>[49]</sup>



b 水滴在超疏水柱状阵列表面的照片及超疏水柱状阵列的SEM照片<sup>[50]</sup>



c “铠甲”超疏水表面在磨损前和磨损后疏水机理的示意图<sup>[54]</sup>

图 11 利用其他方法制造超疏水表面

Fig.11 Fabrication of superhydrophobic surfaces by other methods: a) image of the water droplets on the surface of superhydrophobic aluminum alloy plate and SEM image of the superhydrophobic aluminum alloy plate surface<sup>[49]</sup>; b) image of the water droplets on the superhydrophobic pillar arrays and SEM image of the superhydrophobic pillar arrays<sup>[50]</sup>; c) schematic diagram of hydrophobic mechanism of superhydrophobic surface of the armoured superhydrophobic surface repels water, before and after abrasion<sup>[54]</sup>

### 3 超疏水表面的主要应用

超疏水表面对水表现出优异的排斥性,这种特殊性能使其在自清洁<sup>[56-58]</sup>、防雾<sup>[59-61]</sup>、抗结冰<sup>[62-64]</sup>、耐腐蚀<sup>[65-67]</sup>、液体无损转移<sup>[68-70]</sup>、油水分离<sup>[71-73]</sup>等领域有着广阔的应用前景。随着研究人员的不断探索,超疏水表面的应用领域越来越广,尤其是近几年来,超疏水表面的应用已拓展至摩擦发电<sup>[74-76]</sup>、芯片实验室<sup>[77-79]</sup>、液体传感器<sup>[80-82]</sup>等前沿领域。

#### 3.1 自清洁领域

由于超疏水表面对水滴显示出超低粘附性,因此水滴在倾斜的超疏水表面会自由滚动。水滴在超疏水

表面滚动时,可带走表面的污染物,进而实现超疏水表面的自清洁功能。Shi 等<sup>[56]</sup>将铜片浸泡在温度为 70 °C 的硝酸银溶液中,加热 20 min,经低表面能修饰后获得超疏水铜表面。如图 12a 所示,以粉笔灰作为污染物,滚动的水滴可带走超疏水铜表面的粉笔灰。Liu 等<sup>[57]</sup>采用电化学沉积法在镁合金表面构建微观粗糙结构,再经低表面能修饰后得到超疏水镁合金表面。如图 12b 所示,以碳粉作为污染物,滚动的水滴可带走超疏水镁合金表面的碳粉。Peng 等<sup>[58]</sup>利用喷涂法将经低表面能修饰的氧化锌纳米粒子和二氧化硅纳米粒子通过粘接剂固定在玻璃表面,喷涂后的玻璃表面具有超疏水性。如图 12c 所示,以细砂作为污染物,滚动的水滴可带走超疏水玻璃表面的细砂。

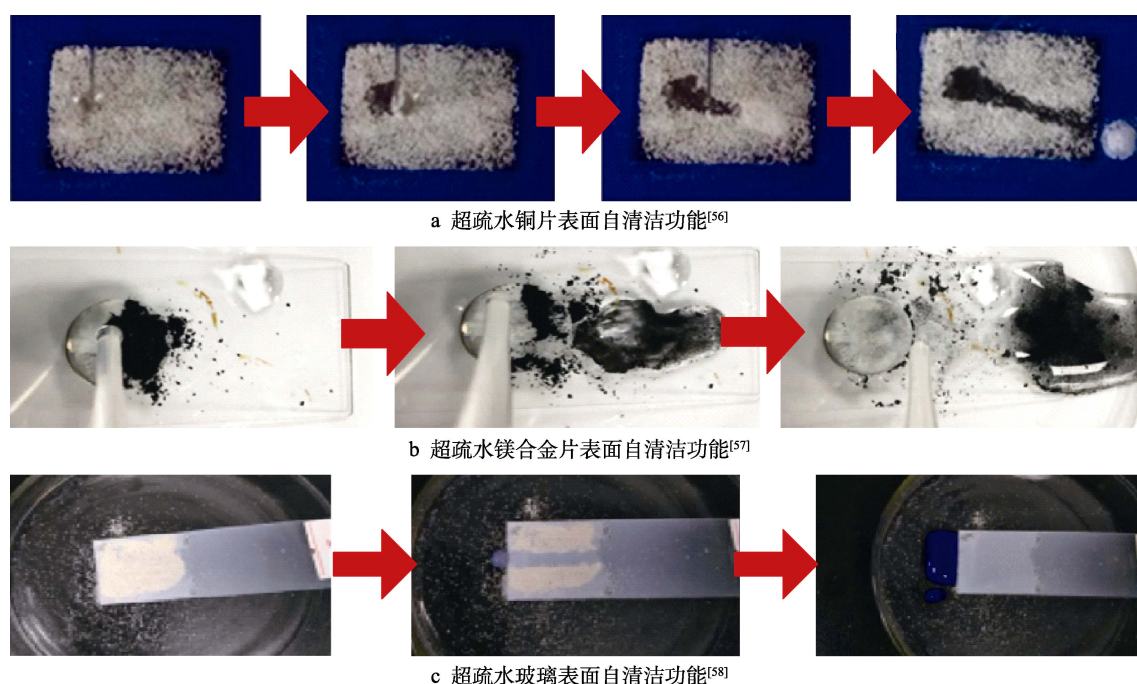


图 12 超疏水表面在自清洁领域的应用

Fig.12 Application of the superhydrophobic surfaces in self-cleaning: a) self-cleaning performance of the superhydrophobic copper plate surface<sup>[56]</sup>; b) self-cleaning function of the superhydrophobic magnesium alloy plate surface<sup>[57]</sup>; c) self-cleaning function of the superhydrophobic glass surface<sup>[58]</sup>

#### 3.2 防雾领域

由于超疏水表面对水表现出优异的排斥性,水滴在其表面易滚落,使超疏水表面在防雾领域有着广阔的应用前景。Gao 等<sup>[59]</sup>发现雾滴在蚊子复眼表面极易滚走,使复眼处于多雾气的环境中长时间不被润湿(图 13a),该小组通过模仿蚊子复眼制作出由 PDMS 半球(图 13b)及二氧化硅纳米球(图 13c)组成的人工复眼,由于二氧化硅纳米球的尺寸小于雾滴尺寸,因此雾滴无法进入人工复眼的纳米结构中,这种独特的微纳米结构使人工复眼具有防雾特性。Sun 等<sup>[60]</sup>研究发现,绿蝇处于潮湿的环境中复眼仍会保持不被润湿(图 13d),基于这一发现,该课题组模仿绿蝇复眼制作出氧化锌(ZnO)纳米粒子(图 13e),

喷涂该 ZnO 纳米粒子的玻璃表面(图 13f)表现出优异的防雾特性。Feng 等<sup>[61]</sup>先在玻璃表面粘接一层具有锥状结构的聚合物涂层,随后在涂层表面喷涂二氧化硅纳米颗粒,并进行低表面能修饰。由于锥状结构和二氧化硅纳米颗粒均为纳米级尺寸,雾滴无法进入涂层的微观结构中,因此得到的超疏水玻璃表面具有防雾性能。

#### 3.3 抗结冰领域

水滴在固体表面的接触角越大,结冰时的热力学势垒越大,活化率越低,水滴的液核越难生成<sup>[83]</sup>。超疏水表面虽不能抑制冰的最终形成,但能延长结冰时间的特性使超疏水表面在抗结冰领域有着广阔的应用前景。Wang 等<sup>[62]</sup>向 PDMS 中加入单壁碳纳米管



(CNT), 并利用纳秒激光加工器在所得的 PDMS/CNT 复合材料表面刻蚀出柱状纹理结构, 如图 14 所

示。与光滑的金属表面 (图 14a)、光滑的 PDMS 表面 (图 14b) 和光滑的 PDMS/CNT 复合材料表面 (图

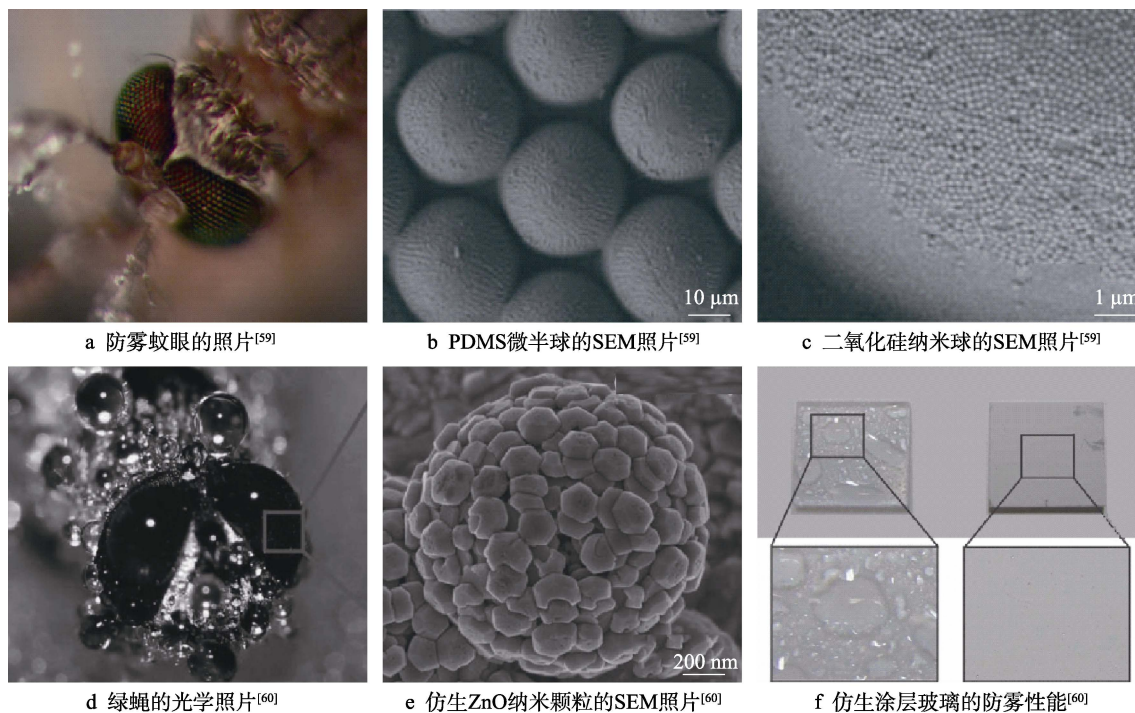


图 13 超疏水表面在防雾领域的应用

Fig.13 Application of the superhydrophobic surfaces in anti-fogging: a) optical photograph of the anti-fogging mosquito eyes<sup>[59]</sup>; b) SEM image of the PDMS micro-hemispheres<sup>[59]</sup>; c) SEM image of the silica nanospheres<sup>[59]</sup>; d) optical image of the green bottle fly<sup>[60]</sup>; e) SEM image of the bio-inspired ZnO nanoparticle<sup>[60]</sup>; f) anti-fogging function of the bio-inspired coating glass<sup>[60]</sup>

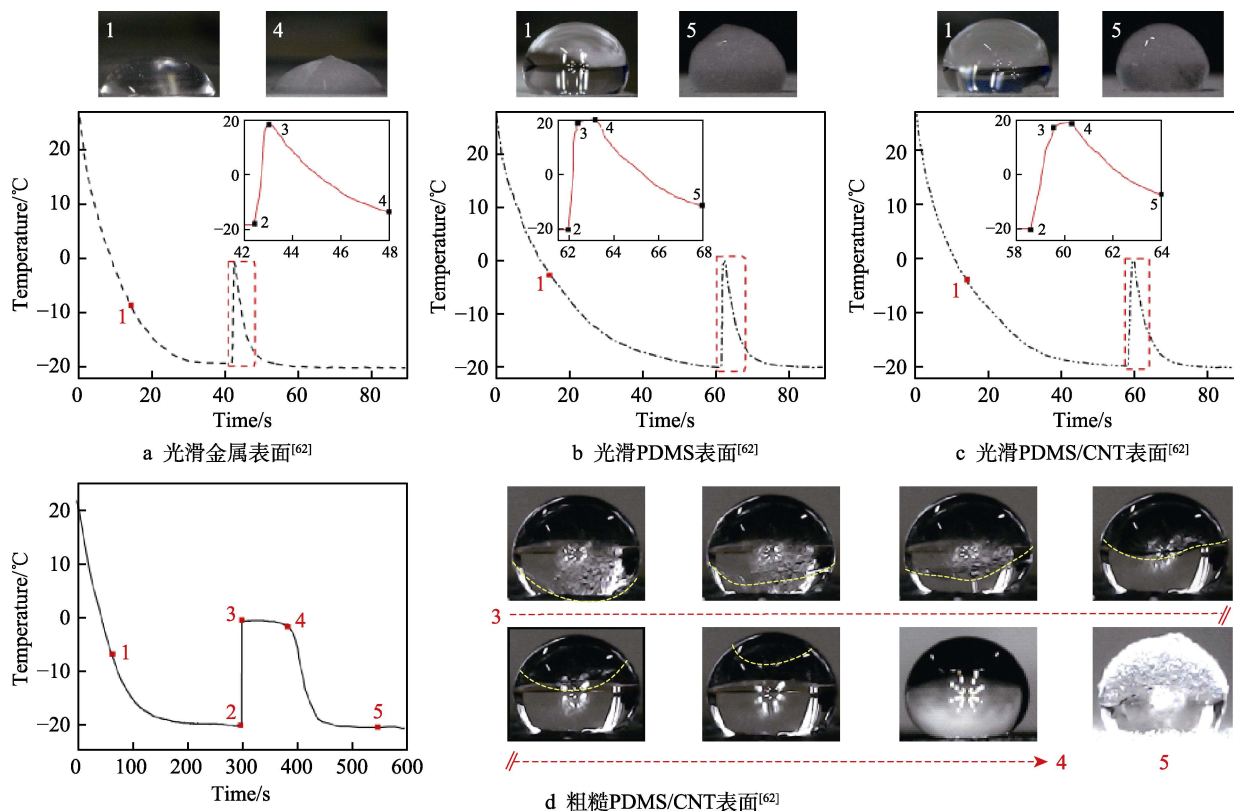


图 14 超疏水表面在抗结冰领域的应用

Fig.14 Application of the superhydrophobic surfaces in anti-icing: a) bare Kanthal-based alloy surface<sup>[62]</sup>; b) neat PDMS surface<sup>[62]</sup>; c) smooth PDMS/CNT surface<sup>[62]</sup>; d) rough PDMS/CNT surface<sup>[62]</sup>



14c) 相比, 粗糙的 PDMS/CNT 复合材料表面 (图 14d) 可大幅延缓结冰时间。Chu 等<sup>[63]</sup>在石墨烯表面制备了纳米分层结构膜, 经低表面能修饰后得到超疏水石墨烯表面, 相对于普通石墨烯表面, 结冰时间从 124 s 延长至 498 s。Xing 等<sup>[64]</sup>利用皮秒激光加工器在铝合金表面构建微观粗糙结构, 经低表面能修饰后, 获得超疏水铝合金表面, 相对于普通铝合金表面, 其结冰时间从 2868 s 延长至 4015 s。

### 3.4 耐腐蚀领域

由于超疏水表面的微观结构可捕获大量空气, 当超疏水表面浸入液体中时, 会在固体表面和液体间形成一层空气垫, 避免液体与固体表面大面积接触, 有效阻止电子的转移, 降低超疏水表面的腐蚀速率, 实现超疏水表面的耐腐蚀功能<sup>[2]</sup>。Feng 等<sup>[65]</sup>通过水热法在铝合金片表面获得微观粗糙结构, 经低表面能修饰后, 获得超疏水铝合金表面。将未经处理的铝合金片 (图 15a 上方) 和超疏水铝合金片 (图 15a 下方) 浸

泡在 3.5%NaCl 溶液中 90 d 后, 观察样品表面变化。可以看出, 未经处理的铝合金表面与 NaCl 溶液大面积接触发生电化学腐蚀, 生成大量白色的腐蚀产物, 而超疏水铝合金表面无明显变化。Wan 等<sup>[66]</sup>通过氯化铈溶液浸泡和低表面能修饰, 在铝片表面获得超疏水二氧化铈涂层, 图 15b 为超疏水铝片耐腐蚀示意图及极化曲线。极化曲线显示, 该超疏水涂层表面的自腐蚀电流密度 ( $4.765 \times 10^{-8} \text{ A/cm}^2$ ) 要比普通铝表面 ( $2.731 \times 10^{-5} \text{ A/cm}^2$ ) 低 3 个数量级, 表明该超疏水涂层能有效地提高铝片的耐腐蚀性。Xun 等<sup>[67]</sup>先将镁合金片浸泡在低浓度硫酸锰溶液中, 随后浸泡在高浓度硫酸锰溶液中, 取出后对镁合金片进行低表面能修饰, 最终获得了超疏水镁合金片。图 15c 为超疏水镁合金片耐腐蚀示意图及极化曲线。极化曲线显示, 超疏水镁合金表面的自腐蚀电流密度 ( $2.703 \times 10^{-8} \text{ A/cm}^2$ ) 要比普通镁合金表面 ( $1.222 \times 10^{-6} \text{ A/cm}^2$ ) 低 2 个数量级, 表明该超疏水表面能有效地提高镁合金片的耐腐蚀性。

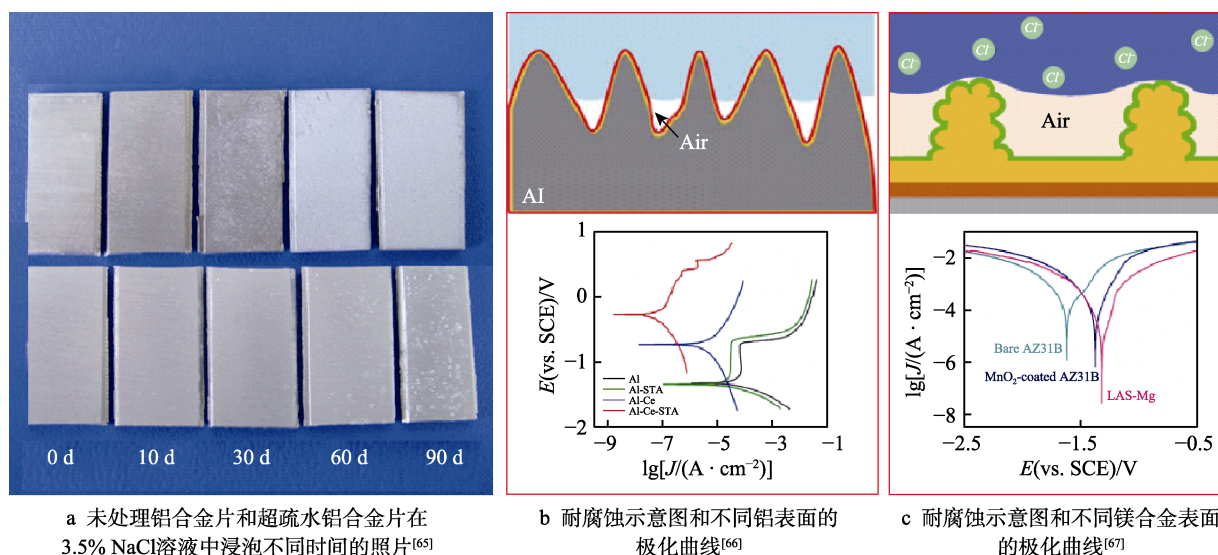


图 15 超疏水表面在耐腐蚀领域的应用

Fig.15 Application of the superhydrophobic surfaces in corrosion resistance: a) the image of the untreated aluminum alloy plate and the superhydrophobic aluminum alloy plate immersed in 3.5% of NaCl solution for different time<sup>[65]</sup>; b) schematic diagram of the corrosion resistance and polarization curves of different aluminum surfaces<sup>[66]</sup>; c) schematic diagram of the corrosion resistance and polarization curves of different magnesium alloy surfaces<sup>[67]</sup>

### 3.5 液体无损转移领域

研究人员发现, 水滴虽然不能进入玫瑰花瓣表面的纳米结构中, 但可以进入较大的微米级粗糙结构, 所以同时具有超疏水性和高粘附性, 此类高粘附超疏水表面在液体无损转移领域有着广阔的应用前景<sup>[68]</sup>。Feng 等<sup>[68]</sup>首次利用模板法复刻玫瑰花瓣表面的微观结构得到了聚合物纳米薄膜, 如图 16a 所示, 水滴只能进入薄膜表面较大的乳突结构, 而无法进入更小的纳米结构中, 即使薄膜表面翻转水滴也不会掉落 (如图 16b 所示)。Wang 等<sup>[69]</sup>利用微波等离子体辅助化学

沉积法合成了一种超疏水金刚石微球, 将该超疏水金刚石微球用环氧树脂粘接在注射器针头上, 如图 16c 所示, 水滴只能进入涂层表面较大的微结构中, 而很难进入更微小的微结构内。相对于普通的注射器针头 (图 16d), 具有金刚石微球涂层的注射器针头 (图 16e) 显示出超疏水性和高粘附性, 可实现对微小液滴的无损转移。Li 等<sup>[70]</sup>将锌箔置于 150 °C 的硝酸锌溶液中反应 18 h, 使锌箔表面生成氧化锌纳米棒结构, 锌箔表面经低表面能修饰后得到超疏水表面。由于水滴只能进入锌箔表面较大的微结构中, 而无法进入纳米级微结构中, 因此该超疏水表面表现出高粘附

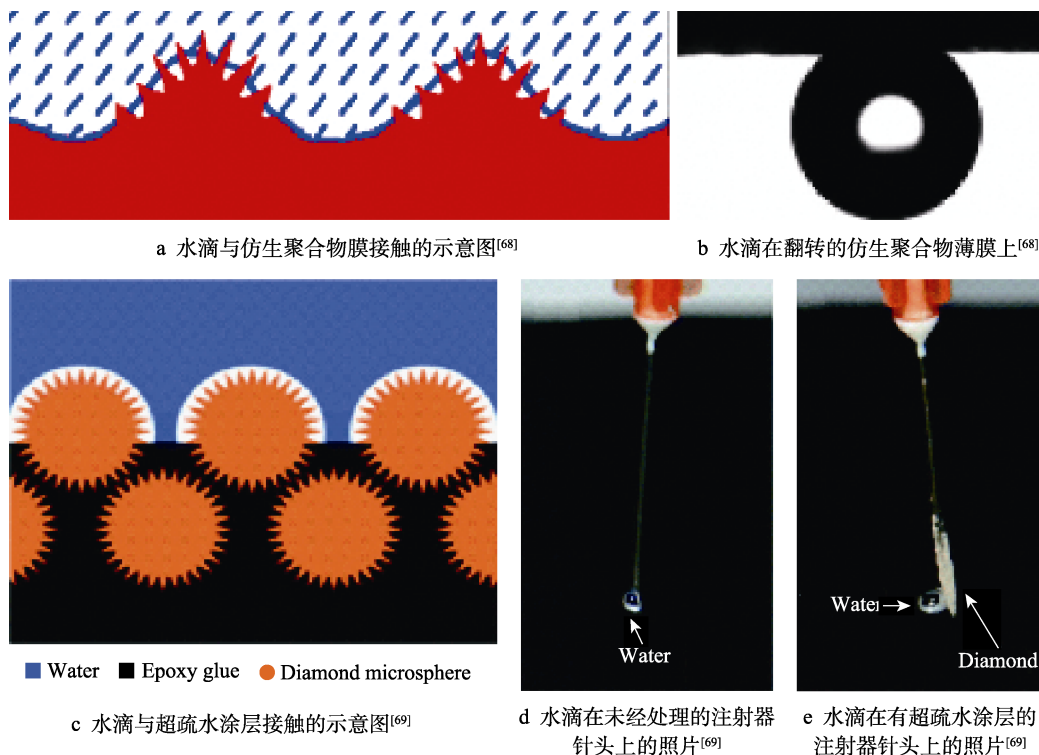


图 16 超疏水表面在液体无损转移领域的应用

Fig.16 Application of the superhydrophobic surfaces in lossless transport of liquid: a) schematic diagram of a water droplet in contact with the biomimetic polymer film<sup>[68]</sup>; b) a water droplet on the biomimetic polymer film when it is turned upside down<sup>[68]</sup>; c) schematic diagram of a water droplet in contact with the composite superhydrophobic coating<sup>[69]</sup>; d) optical image of a water droplet hanging on an untreated syringe needle<sup>[69]</sup>; e) optical image of a water droplet hanging on a syringe needle with the superhydrophobic coating<sup>[69]</sup>

性。该课题组以此类高粘附超疏水铝箔表面作为机械手,将低粘附超疏水铝表面上的水滴无损转移至亲水硅片表面上。

### 3.6 油水分离领域

研究人员发现,水和油的表面张力存在差异,水的表面张力约为 72.8 mN/m,而大部分油的表面张力都小于 40 mN/m。若超疏水表面的表面张力介于水和油之间,就可同时具有超疏水和超亲油的性能,使超疏水表面实现油水分离功能<sup>[84]</sup>。Liu 等<sup>[71]</sup>通过一步浸泡法将普通聚氨酯海绵浸泡在硬脂酸铜乙醇溶液中,得到超疏水-超亲油海绵(图 17a),但是海绵的储存能力有限,其吸油量受到很大限制。因此该小组设计了一种由超疏水-超亲油海绵和玻璃容器组成的吸油器(图 17b),与仅使用海绵吸油相比,吸油器不需要实验人员手动挤压海绵及浮油回收。吸油器使用如图 17c 所示,浮油首先会被超疏水-超亲油海绵吸收,随后油在海绵内会由于重力向下流动,最终流入吸油器的玻璃容器内,完成油水分离。Qin 等<sup>[72]</sup>通过皮秒激光加工器在聚四氟乙烯(PTFE)表面加工出微纳米粗糙结构及微孔结构,由于 PTFE 自身为低表面能材料,无需进行低表面能修饰即可获得超疏水-超亲油 PTFE 表面;由于 PTFE 表面超疏水-超亲油的特性,油滴接触到 PTFE 表面后,会从 PTFE 表面的微孔结

构中通过,而水滴则无法通过 PTFE 表面,油水分离效率超过 99%。图 17d 为超疏水聚四氟乙烯膜制备工艺及油水分离示意图。Liu 等<sup>[73]</sup>将聚酯纤维(PET)织物浸泡在氢氧化钠溶液中进行化学刻蚀,经低表面能修饰后,获得具有超疏水-超亲油性能的 PET 织物。该超疏水-超亲油 PET 织物浸入油水混合物后,油会由于表面张力被 PET 织物吸收,水则无法进入 PET 织物。该 PET 织物具有优异的吸油能力,可吸附自身质量 48~73 倍的油(具体差异取决于油的表面张力、密度和黏度)。

### 3.7 摩擦发电领域

近年来,研究人员发现,液体在固体表面滚动会导致毗邻固体表面的液体分子与固体表面的原子产生电子云交叠,实现电子转移。当液体从固体表面脱离后,固体表面带负电,与固体接触的金属电极会产生感应电荷,金属电极与地面相接后产生电位差,电子从低电位向高电位流动,产生电流<sup>[85]</sup>。若液体不能从固体表面完全脱离,则会降低金属电极与地面之间的电位差,降低发电功率,而超疏水表面对水滴显示出超低粘附性,水滴在倾斜的超疏水表面极易滚落,因此超疏水表面被认为是理想的摩擦发电材料<sup>[74]</sup>。Lin 等<sup>[75]</sup>在聚四氟乙烯薄膜(PTFE)表面加工出微纳米级粗糙结构,由于 PTFE 自身为低表面能材料,无

需进行低表面能修饰, 即可获得超疏水 PTFE 表面, 将 PTFE 薄膜附在涂有铜电极的聚甲基丙烯酸甲酯

(PMMA) 基板上。图 18 为超疏水表面产生电能示意图。水滴从超疏水 PTFE 薄膜表面滚落后, 铜电极

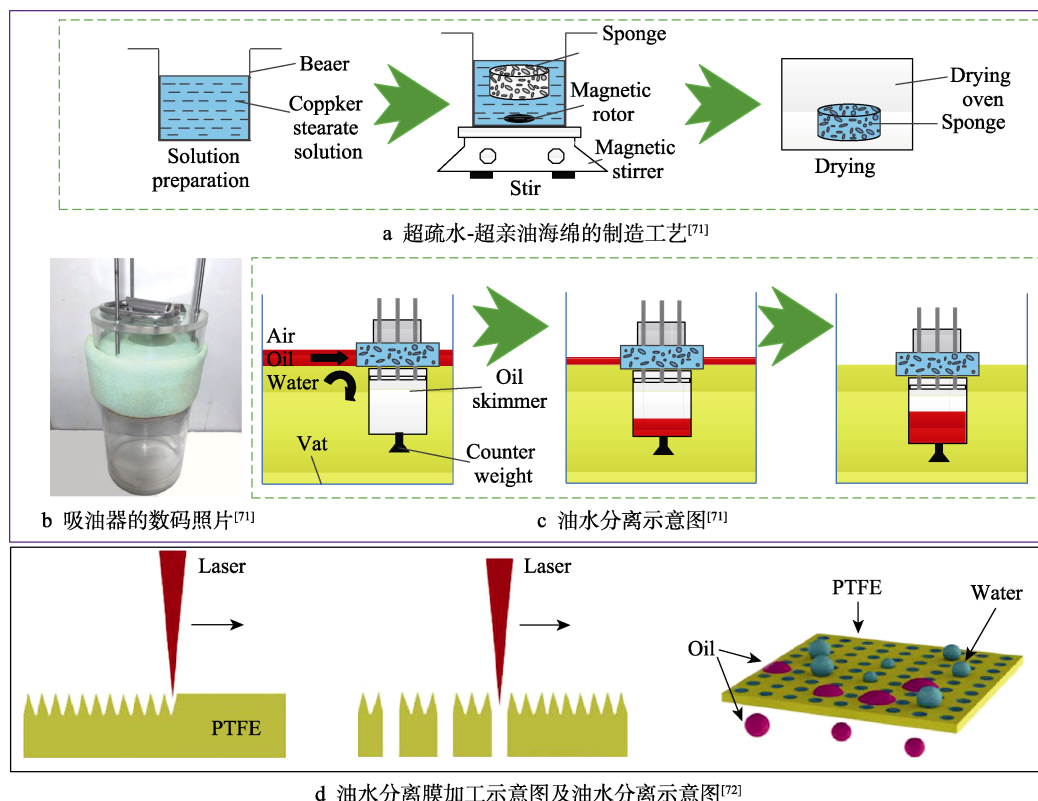


图 17 超疏水表面在油水分离领域的应用

Fig.17 Application of the superhydrophobic surfaces in oil-water separation: a) fabrication processes of the superhydrophobic-superoleophilic sponges<sup>[71]</sup>; b) digital photo of the oil skimmer<sup>[71]</sup>; c) schematics of the oil-water separation<sup>[71]</sup>; d) fabrication processes of the oil-water separation membranes and schematic diagram of the oil-water separation<sup>[72]</sup>

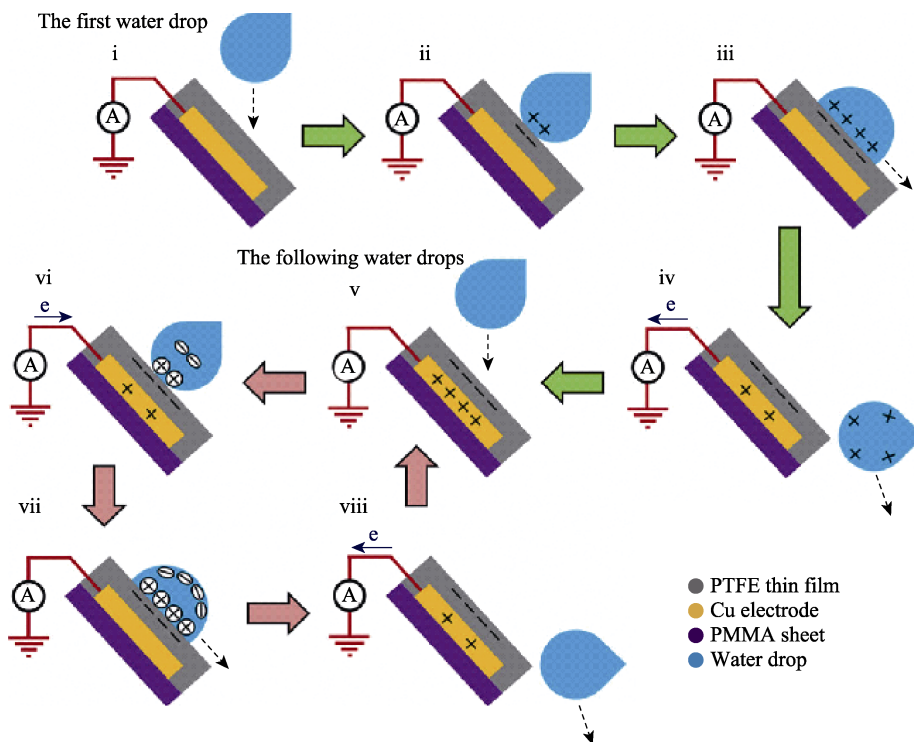


图 18 超疏水表面在摩擦发电领域的应用: 超疏水表面产生电能示意图<sup>[75]</sup>

Fig.18 Application of the superhydrophobic surfaces in triboelectric nanogenerator: Schematic illustrations of the generating electricity on superhydrophobic surface<sup>[75]</sup>



受 PTFE 薄膜上负电荷的影响产生感应电荷,电子从铜电极流向地面产生电流。当下一滴水接触超疏水 PTFE 薄膜时,水滴与 PTFE 薄膜建立电平衡,铜电极不再受 PTFE 薄膜影响,因此铜电极与地面产生电势差,电子从地面流向铜电极产生电流。水滴离开 PTFE 薄膜表面时,铜电极与地面之间将产生电位差,电子从铜电极流向地面产生电流。Cho 等<sup>[76]</sup>发现普通超疏水表面纳米结构内的空气垫较薄,当水滴高速接触超疏水表面时,空气垫易破裂,导致部分微小的水滴渗入纳米结构内,不会从超疏水表面滚落,若微小的水滴逐渐累积,则会导致无电流输出。该课题组针对此问题,设计了一种具有层次结构的超疏水表面,表面形成了较厚的空气垫,防止水滴渗入到微观结构底部,当下一滴水接触该超疏水表面时,会带走存留的微小水滴,使得具有层次结构的超疏水表面输出电能更稳定。

### 3.8 芯片实验室

近年来,高度集成的芯片实验室设备在生物、化学等领域发挥着举足轻重的作用,然而残留液滴易粘

附在设备表面,造成芯片实验室设备的污染。超疏水表面对水滴显示出超低粘附性,避免了水滴在超疏水表面的残留,因此超疏水表面在芯片实验室领域有着广阔的应用前景<sup>[77]</sup>。Accardo 等<sup>[78]</sup>设计并制造了一种超疏水液滴混合装置,如图 19a 所示。施加外部电位,会改变水滴在超疏水表面的润湿性,可使两滴水混合为一滴大水滴(图 19b)。该液滴混合装置的超疏水表面具有超低的粘附力,避免了混合过程中液滴在固体表面的残留,在芯片实验室的微量液滴混合方面有着广阔的应用前景。Dong 等<sup>[79]</sup>利用电火花加工技术在钛片表面加工出复杂的轨道,随后利用电化学刻蚀法在钛片表面刻蚀出微纳米级的粗糙结构,最后经低表面能修饰后,获得可定向运输水滴的超疏水表面,如图 19c 所示。将制备的超疏水钛片固定在倾斜角为  $5^\circ$  的斜面上,水滴会在重力的作用下沿着超疏水表面上的轨道滚动,实现水滴的定向运输。水滴从该超疏水轨道表面滚落后,轨道表面没有微小的水滴粘附,说明该超疏水轨道表面对水具有超低的粘附性,为今后芯片实验室液滴引导轨道的制备提供了新思路。

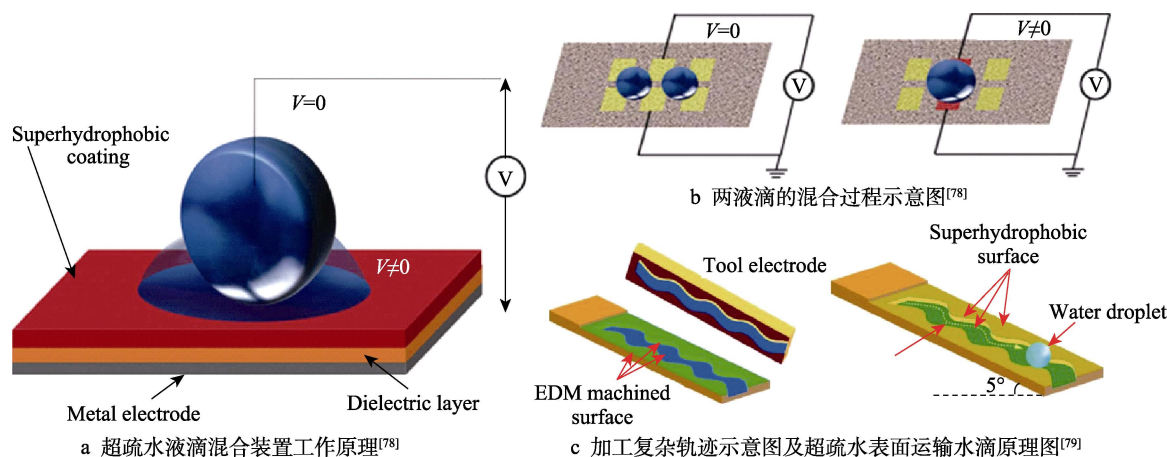


图 19 超疏水表面在芯片实验室领域的应用

Fig.19 Application of the superhydrophobic surfaces in lab-on-a-chip: a) principle of the superhydrophobic droplet mixing device<sup>[78]</sup>; b) schematic diagram of the coalescence process of two droplets<sup>[78]</sup>; c) schematic diagram of manufacturing complex trajectory and schematic illustration of the water droplet transported on the superhydrophobic surface<sup>[79]</sup>

### 3.9 液滴传感器

近年来,研究人员在研究液体与固体摩擦发电的过程中,发现液滴从超疏水表面滚落会产生摩擦电效应,而由于摩擦电效应产生的电信号可用于检测液滴的流量,在液滴传感器领域有着广阔的应用前景<sup>[80]</sup>。Chen 等<sup>[81]</sup>根据液/固界面的摩擦电效应会产生电信号的原理,设计了一种摩擦电液滴传感器,如图 20a 所示。该液滴传感器可用于医院病人输液或工业生产中液滴流速的实时检测,该液滴传感器在不同注射速度条件下,会产生不同频率的电信号,由此可计算出液滴的间隔时间,如图 20b 所示。此外,通过记录输出电信号峰的数量,还可计算出一定时间内流出药液的量。Hu 等<sup>[82]</sup>设计并制造了一种由超疏水表面和硅

橡胶管组成的管状液滴传感器(图 20c),液滴从管状液滴传感器的超疏水表面滚落,会产生脉冲电流,通过调节速度控制阀可检测到不同的电流信号,如图 20d 所示。利用该管状液滴传感器可有效且精确地计算液滴滴落量。

### 3.10 其他领域

此外,超疏水表面在阻燃<sup>[86-88]</sup>、响应开关<sup>[89-91]</sup>、流体减阻<sup>[92-94]</sup>等领域也具有广阔的应用前景。Chen 等<sup>[86]</sup>以羟基磷灰石纳米线为材料制备无机纸,该无机纸经低表面能修饰后获得超疏水性。由于羟基磷灰石纳米线具有优异的阻燃性,因此所制备的超疏水无机纸具有优异的阻燃性。如图 21a 所示。Yang 等<sup>[91]</sup>利用喷涂法和磁场定向自组装技术,制造了一种由磁响

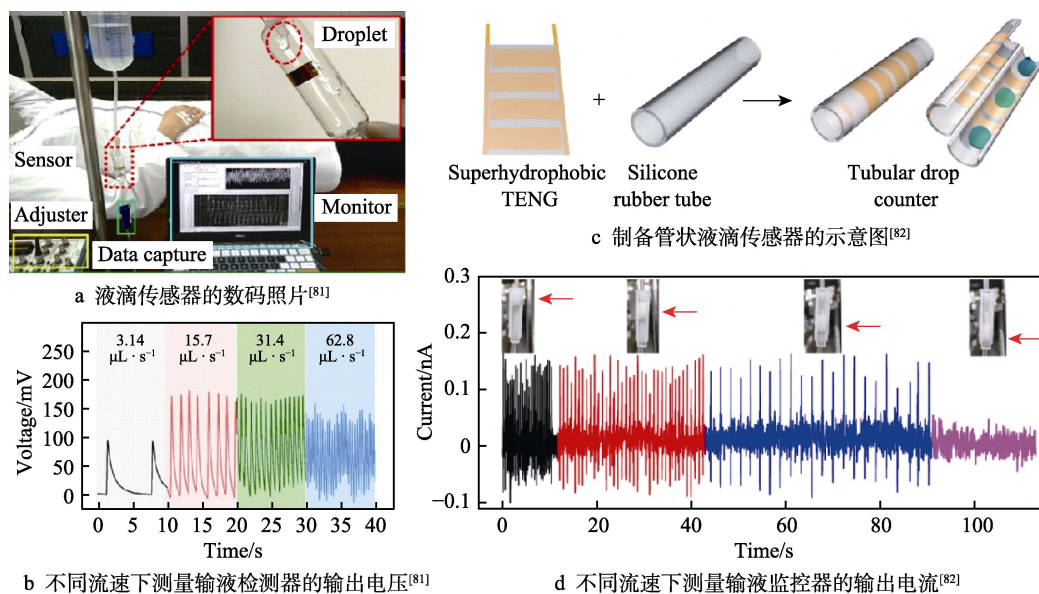


图 20 超疏水表面在液滴传感器领域的应用

Fig.20 Application of the superhydrophobic surfaces in droplet sensor: a) digital photo of the droplet flow sensor<sup>[81]</sup>; b) output voltage of the infusion monitor measured at different flow rates<sup>[81]</sup>; c) schematic illustration of preparing the tubular droplet sensor<sup>[82]</sup>; d) output current of the infusion monitor measured at different flow rates<sup>[82]</sup>

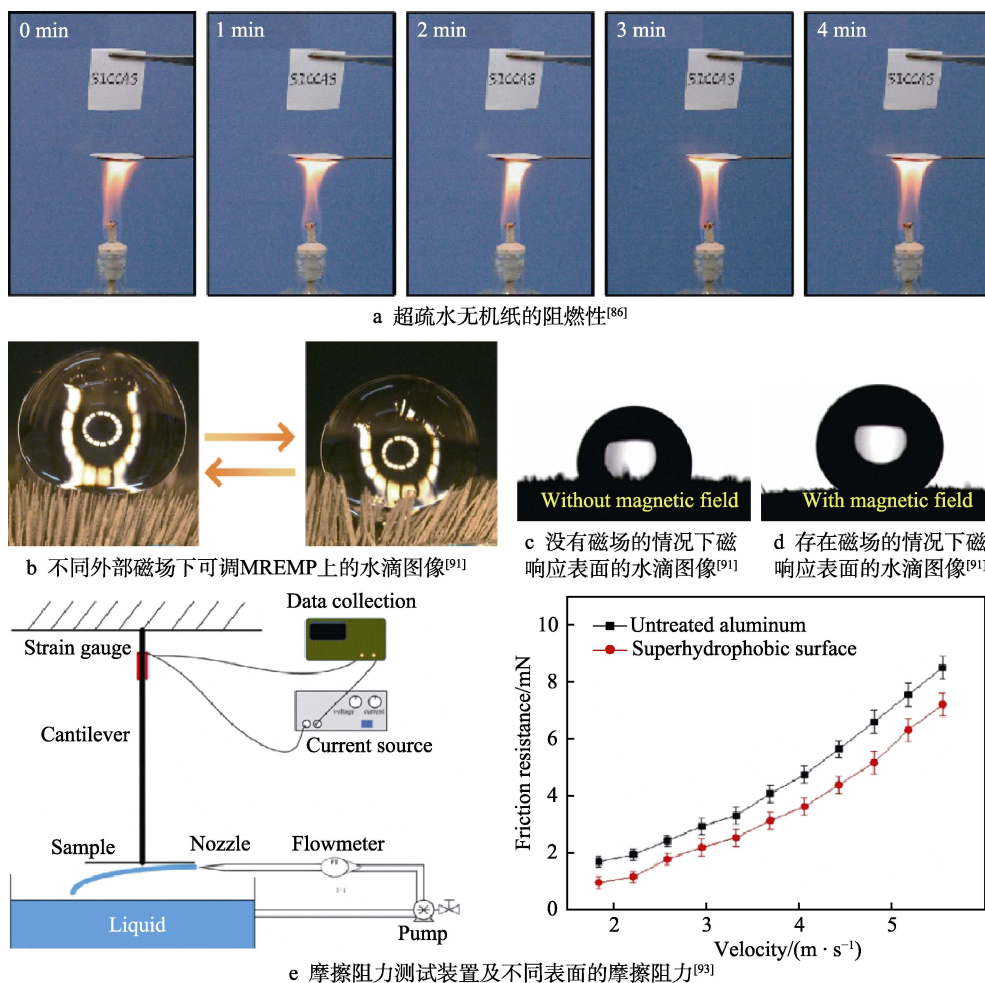


图 21 超疏水表面在其他领域的应用

Fig.21 Application of the superhydrophobic surfaces in other fields: a) the fire-resistant of superhydrophobic inorganic paper<sup>[86]</sup>; b) images of the water droplet on the tunable MREMPs under different external magnet field<sup>[91]</sup>; c) image of a water droplet on the magnetically responsive surface in the absence magnetic field<sup>[91]</sup>; d) image of a water droplet on the magnetically responsive surface in the presence magnetic field<sup>[91]</sup>; e) the testing device of the friction resistance and the friction resistance of different surfaces<sup>[93]</sup>

应弹性微柱 (MREMP) 阵列组成的表面, 在不同磁场作用下, 该表面的润湿性呈现可逆切换的特性, 如图 21b 所示。在没有磁场的情况下, 由于 MREMP 具有弹性, 易在液滴载荷的作用下产生弯曲, 此时液滴与表面接触角约为  $105.6^\circ$  (图 21c); 在有磁场的情况下, 表面的 MREMP 变硬, 其抗弯刚度显著提高, 此时液滴与表面之间接触角约为  $150.9^\circ$  (图 21d)。Tuo 等<sup>[93]</sup>利用水热法在铝箔表面制备了一层超疏水薄膜, 水滴与超疏水铝箔表面的接触状态为 Cassie-Baxter 模式, 水流同时与铝箔表面、空气接触, 形成由固-液-气三相组成的复合接触面。由于水流与固体之间的摩擦阻力比水流与空气之间的摩擦阻力大, 因此超疏水铝箔表面相对于普通铝箔表面具有减阻功能, 减阻在 20~30%, 图 21e 为阻力测试装置及不同表面的摩擦阻力曲线图。

## 4 结论与展望

近年来, 研究人员通过激光刻蚀法、化学沉积法、化学刻蚀法、电化学沉积法、电化学刻蚀法、热氧化法、喷涂法等不同的加工手段及制备方法制备出多种超疏水表面。超疏水表面因其优异的疏水特性, 被广泛地应用于自清洁、防雾、抗结冰、耐腐蚀、液体无损转移、油水分离、摩擦发电、芯片实验室、液滴传感器等领域。此外, 研究人员针对超疏水表面现存的不能大面积制造、低表面能修饰材料价格昂贵且对环境有污染、超疏水表面机械强度差等问题做了许多研究工作, 例如: Song 等<sup>[50]</sup>利用模板法大面积制造具有超疏水性能的柱状阵列表面; Liu 等<sup>[22]</sup>通过构建双凹角结构, 无需进行低表面能修饰就可实现超疏水状态; Deng 等<sup>[54]</sup>首次设计并制造了具有“铠甲”结构的超疏水表面, 相对于传统的超疏水表面, “铠甲”结构的超疏水表面极大地提高了机械强度。但是, 目前超疏水表面的制造和应用仍停留在实验研究阶段, 从实验室研究走向工业化应用还存在很多问题:

1) 目前大面积制造超疏水表面存在工艺流程繁琐、制备成本高等问题, 因此需要进一步研究可高效、低成本的大面积制造超疏水表面的加工方法。

2) 现有的低表面能修饰材料价格昂贵且对环境有污染, 虽然近年来有研究人员通过构建特殊的微观结构, 达到无需进行低表面能修饰就可实现超疏水, 但是加工设备昂贵, 生产成本低。因此, 需要进一步开发经济环保的低表面能修饰剂, 或开发通过经济、简单的加工方法即可得到特殊的微观结构, 以达到无需进行低表面能修饰即可实现超疏水状态的效果。

3) 超疏水表面的微纳米级粗糙结构易受到摩擦、冲击等机械破坏, 使超疏水表面失去超疏水性能。虽然近年来有研究人员研制出高机械强度的超疏水表面, 但是工艺繁琐, 制造成本高, 因此需要进一步研究如何低成本制造高机械强度的超疏水表面。

4) 进一步拓展超疏水表面的多功能性及实际应用性, 加强超疏水表面在工业中的应用基础研究, 满足不断提高的应用需求。

## 参考文献:

- [1] 江雷. 从自然到仿生的超疏水纳米界面材料[J]. 化工进展, 2003, 22(12): 1258-1264.  
JIANG Lei. Nanostructured materials with superhydrophobic surface—From nature to biomimesis[J]. Chemical industry and engineering progress, 2003, 22(12): 1258-1264.
- [2] 宋金龙, 陆遥, 黄帅, 等. 极端润湿性表面研究与应用进展[J]. 科技导报, 2015, 33(15): 92-100.  
SONG Jin-long, LU Yao, HUANG Shuai, et al. Progress on research and application of extreme wettability surfaces[J]. Science & technology review, 2015, 33(15): 92-100.
- [3] BARTHOLOTT W, NEINHUIS C. Purity of the sacred lotus, or escape from contamination in biological surfaces[J]. Planta, 1997, 202(1): 1-8.
- [4] FENG L, LI S, LI Y, et al. Super-hydrophobic surfaces: From natural to artificial[J]. Advanced materials, 2002, 14(24): 1857-1860.
- [5] YOUNG T. An essay on the cohesion of fluids[J]. Philosophical Transactions of the Royal Society of London, 1805, 95: 65-87.
- [6] WENZEL R N. Resistance of solid surfaces to wetting by water[J]. Industrial & engineering chemistry, 1936, 28(8): 988-994.
- [7] CASSIE A B D, BAXTER S. Wettability of porous surfaces[J]. Transactions of the Faraday Society, 1944, 40: 546-551.
- [8] FU C, GU L, ZENG Z X, et al. One-step transformation of metal meshes to robust superhydrophobic and superoleophilic meshes for highly efficient oil spill cleanup and oil/water separation[J]. ACS applied materials & interfaces, 2020, 12(1): 1850-1857.
- [9] NIU S, SUN C, TANG B W, et al. Preparation and superhydrophobicity of Sn thin film based Zn substrate[J]. Integrated ferroelectrics, 2019, 199(1): 52-57.
- [10] SUN J, CHENG W, SONG J L, et al. Fabrication of superhydrophobic micro post array on aluminum substrates using mask electrochemical machining[J]. Chinese journal of mechanical engineering, 2018, 31(1): 72.
- [11] SHEN C, ZHAN Y J, ZHU Y Q, et al. Preparation of smart glass with superhydrophobic and thermochromic properties[J]. Chemical physics letters, 2019, 723: 65-68.
- [12] XU M, FENG Y, LI Z L, et al. A novel, efficient and cost-effective synthesis technique for the development of superhydrophobic glass surface[J]. Journal of alloys and compounds, 2019, 781: 1175-1181.
- [13] ZHU J Y, LIAO K J. Preparation of superhydrophobic surface with tunable adhesion on glass substrate[J]. Ma-



- terials research express, 2020, 7(7): 076409.
- [14] XU L Y, LAI Y L, LIU L, et al. The effect of plasma electron temperature on the surface properties of superhydrophobic cotton fabrics[J]. *Coatings*, 2020, 10(2): 160.
- [15] ROY S, ZHAI L D, KIM J W, et al. A novel approach of developing sustainable cellulose coating for self-cleaning-healing fabric[J]. *Progress in organic coatings*, 2020, 140: 105500.
- [16] 卢永熠, 冯勇鸿, 黄洋, 等. 自修复超疏水抗菌织物的制备和性能研究[J]. *功能材料*, 2020, 7(51): 7110-7116. LU Yong-yi, FENG Yong-hong, HUANG Yang, et al. Preparation and properties of self-healing superhydrophobic antibacterial fabric[J]. *Journal of functional materials*, 2020, 7(51): 7110-7116.
- [17] XU K, REN S Z, SONG J L, et al. Colorful superhydrophobic concrete coating[J]. *Chemical engineering journal*, 2021, 403: 126348.
- [18] ZHU J Y, LIAO K J. A facile and low-cost method for preparing robust superhydrophobic cement block[J]. *Materials chemistry and physics*, 2020, 250: 123064.
- [19] WANG F J, LEI S, OU J F, et al. Superhydrophobic calcium aluminate cement with super mechanical stability [J]. *Industrial & engineering chemistry research*, 2019, 58(24): 10373-10382.
- [20] 鲍田, 王东. 玻璃表面二氧化硅基超疏水膜的研究进展[J]. *表面技术*, 2019, 48(8): 156-164. BAO Tian, WANG Dong. Research progress in silica-based superhydrophobic thin films on glass[J]. *Surface technology*, 2019, 48(8): 156-164.
- [21] 蒋帆, 赵越, 胡吉明. 超疏水表面在金属防护中应用的研究进展[J]. *表面技术*, 2020, 49(2): 109-123. JIANG Fan, ZHAO Yue, HU Ji-ming. Research advance in application of superhydrophobic surfaces in corrosion protection of metals[J]. *Surface technology*, 2020, 49(2): 109-123.
- [22] LIU T Y, KIM C J. Turning a surface superrepellent even to completely wetting liquids[J]. *Science*, 2014, 346(6213): 1096-1100.
- [23] CHECCO A, RAHMAN A, BLACK C T. Robust superhydrophobicity in large-area nanostructured surfaces defined by block-copolymer self assembly[J]. *Advanced materials*, 2014, 26(6): 886-891.
- [24] YUAN S S, ZHU J Y, LI Y, et al. Structure architecture of micro/nanoscale ZIF-L on a 3D printed membrane for a superhydrophobic and underwater superoleophobic surface[J]. *Journal of materials chemistry A*, 2019, 7(6): 2723-2729.
- [25] HUANG S, SONG J L, LU Y, et al. Underwater spontaneous pumpless transportation of nonpolar organic liquids on extreme wettability patterns[J]. *ACS applied materials & interfaces*, 2016, 8(5): 2942-2949.
- [26] LIU Z A, YANG X L, PANG G B, et al. Temperature-based adhesion tuning and superwettability switching on superhydrophobic aluminum surface for droplet manipulations[J]. *Surface and coatings technology*, 2019, 375: 527-533.
- [27] ZHANG Q Q, ZHANG H C. Corrosion resistance and mechanism of micro-nano structure super-hydrophobic surface prepared by laser etching combined with coating process[J]. *Anti-corrosion methods and materials*, 2019, 66(3): 264-273.
- [28] YONG J L, CHEN F, YANG Q, et al. Femtosecond laser weaving superhydrophobic patterned PDMS surfaces with tunable adhesion[J]. *The journal of physical chemistry C*, 2013, 117(47): 24907-24912.
- [29] HUANG L, SONG J L, LU Y, et al. Superoleophobic surfaces on stainless steel substrates obtained by chemical bath deposition[J]. *Micro & nano letters*, 2017, 12(2): 76-81.
- [30] JIA J, FAN J F, XU B S, et al. Microstructure and properties of the super-hydrophobic films fabricated on magnesium alloys[J]. *Journal of alloys and compounds*, 2013, 554: 142-146.
- [31] ZHU J Y, ZHANG L P, DAI X J, et al. One-step fabrication of a superhydrophobic copper surface by nano-silver deposition[J]. *AIP advances*, 2020, 10(7): 075111.
- [32] SALEH T A, BAIG N. Efficient chemical etching procedure for the generation of superhydrophobic surfaces for separation of oil from water[J]. *Progress in organic coatings*, 2019, 133: 27-32.
- [33] XIAO X Y, XIE W, YE Z H. Preparation of corrosion-resisting superhydrophobic surface on aluminium substrate[J]. *Surface engineering*, 2018, 35(5): 411-417.
- [34] LIU W, XU Q J, HAN J, et al. A novel combination approach for the preparation of superhydrophobic surface on copper and the consequent corrosion resistance[J]. *Corrosion science*, 2016, 110: 105-113.
- [35] TAN J Y, HAO J J, AN Z Q, et al. Simple fabrication of superhydrophobic nickel surface on steel substrate via electrodeposition[J]. *International journal of electrochemical science*, 2017, 12(1): 40-49.
- [36] LIU Y, XUE J, LUO D, et al. One-step fabrication of biomimetic superhydrophobic surface by electrodeposition on magnesium alloy and its corrosion inhibition[J]. *Journal of colloid and interface science*, 2017, 491: 313-320.
- [37] SU F, YAO K. Facile fabrication of superhydrophobic surface with excellent mechanical abrasion and corrosion resistance on copper substrate by a novel method[J]. *ACS applied materials & interfaces*, 2014, 6(11): 8762-8770.
- [38] LIU Z A, ZHANG F, CHEN Y, et al. Electrochemical fabrication of superhydrophobic passive films on aeronautic steel surface[J]. *Colloids and surfaces A: Physicochemical and engineering aspects*, 2019, 572: 317-325.
- [39] LU Z, WANG P, ZHANG D. Super-hydrophobic film fabricated on aluminium surface as a barrier to atmospheric corrosion in a marine environment[J]. *Corrosion science*, 2015, 91: 287-296.

- [40] LI X J, YIN S H, HUANG S, et al. Fabrication of durable superhydrophobic Mg alloy surface with water-repellent, temperature-resistant, and self-cleaning properties[J]. Vacuum, 2020, 173: 109172.
- [41] LV Z X, YU S R, SONG K X, et al. Fabrication of a leaf-like superhydrophobic CuO coating on 6061Al with good self-cleaning, mechanical and chemical stability[J]. Ceramics international, 2020, 46(10): 14872-14883.
- [42] CAO L, WAN Y, WANG Y H, et al. Fabrication and mechanical durability of a superhydrophobic copper surface with morphological development from hydrothermal reaction[J]. Surface and interface analysis, 2016, 48(13): 1418-1422.
- [43] 康志新, 郭明杰. 热氧化法制备超疏水 Ti 表面及其耐腐蚀性[J]. 金属学报, 2013, 49(5): 629-634.  
KANG Zhi-xin, GUO Ming-jie. Fabrication of superhydrophobic Ti surface by thermal oxidation and its anti-corrosion property[J]. Acta metallurgica sinica, 2013, 49(5): 629-634.
- [44] DENG W S, LONG M Y, MIAO X R, et al. Eco-friendly preparation of robust superhydrophobic Cu(OH)<sub>2</sub> coating for self-cleaning, oil-water separation and oil sorption[J]. Surface and coatings technology, 2017, 325: 14-21.
- [45] WANG C Z, TANG F, LI Q, et al. Spray-coated superhydrophobic surfaces with wear-resistance, drag-reduction and anti-corrosion properties[J]. Colloids and surfaces A: Physicochemical and engineering aspects, 2017, 514: 236-242.
- [46] LU Y, SATHASIVAM S, SONG J L, et al. Robust self-cleaning surfaces that function when exposed to either air or oil[J]. Science, 2015, 347(6226): 1132-1135.
- [47] DING C D, TAI Y, WANG D, et al. Superhydrophobic composite coating with active corrosion resistance for AZ31B magnesium alloy protection[J]. Chemical engineering journal, 2019, 357: 518-532.
- [48] WANG M, PENG M, WENG Y X, et al. Toward durable and robust superhydrophobic cotton fabric through hydrothermal growth of ZnO for oil/water separation[J]. Cellulose, 2019, 26(13-14): 8121-8133.
- [49] ZHANG B B, WANG J, ZHANG J. Bioinspired one step hydrothermal fabricated superhydrophobic aluminum alloy with favorable corrosion resistance[J]. Colloids and surfaces A: Physicochemical and engineering aspects, 2020, 589: 124469.
- [50] SONG J L, GAO M Q, ZHAO C L, et al. Large-area fabrication of droplet pancake bouncing surface and control of bouncing state[J]. ACS nano, 2017, 11(9): 9259-9267.
- [51] LV D M, SHENG L, WAN J P, et al. Bioinspired hierarchically hairy particles for robust superhydrophobic coatings via a droplet dynamic template method[J]. Polymer chemistry, 2019, 10(3): 331-335.
- [52] XIANG T F, CHEN D P, LV Z, et al. Robust superhydrophobic coating with superior corrosion resistance[J]. Journal of alloys and compounds, 2019, 798: 320-325.
- [53] JIANG H B, Q, LIU Y, ZHANG Y L, et al. Reed leaf-inspired graphene films with anisotropic superhydrophobicity[J]. ACS applied materials & interfaces, 2018, 10(21): 18416-18425.
- [54] WANG D H, SUN Q Q, HOKKANEN M J, et al. Design of robust superhydrophobic surfaces[J]. Nature, 2020, 582(7810): 55-59.
- [55] ZHU J J, TIAN Y L, LIU X P, et al. Lithography-induced hydrophobic surfaces of silicon wafers with excellent anisotropic wetting properties[J]. Microsystem technologies, 2018, 25(2): 735-745.
- [56] SHI X, ZHAO L, WANG J, et al. Toward easily enlarged superhydrophobic copper surfaces with enhanced corrosion resistance, excellent self-cleaning and anti-icing performance by a facile method[J]. Journal of nanoscience and nanotechnology, 2020, 20(10): 6317-6325.
- [57] LIU X, ZHANG T C, HE H Q, et al. A stearic acid/CeO<sub>2</sub> bilayer coating on AZ31B magnesium alloy with superhydrophobic and self-cleaning properties for corrosion inhibition[J]. Journal of alloys and compounds, 2020, 834: 155210.
- [58] PENG J, ZHAO X, WANG W, et al. Durable self-cleaning surfaces with superhydrophobic and highly oleophobic properties[J]. Langmuir, 2019, 35(25): 8404-8412.
- [59] GAO X F, YAN X, YAO X, et al. The dry-style antifogging properties of mosquito compound eyes and artificial analogues prepared by soft lithography[J]. Advanced materials, 2007, 19(17): 2213-2217.
- [60] SUN Z Q, LIAO T, LIU K S, et al. Fly-eye inspired superhydrophobic anti-fogging inorganic nanostructures[J]. Small, 2014, 10(15): 3001-3006.
- [61] FENG C C, ZHANG Z Y, LI J, et al. A bioinspired, highly transparent surface with dry-style antifogging, antifrosting, antifouling, and moisture self-cleaning properties[J]. Macromolecular rapid communications, 2019, 40(6): e1800708.
- [62] WANG F X, TAY T E, SUN Y Y, et al. Low-voltage and surface energy SWCNT/poly(dimethylsiloxane) (PDMS) nanocomposite film: surface wettability for passive anti-icing and surface-skin heating for active deicing[J]. Composites science and technology, 2019, 184: 107872.
- [63] CHU Z M, JIAO W C, HUANG Y F, et al. Smart superhydrophobic films with self-sensing and anti-icing properties based on silica nanoparticles and graphene[J]. Advanced materials interfaces, 2020, 7(15): 2000492.
- [64] XING W, LI Z, YANG H O, et al. Anti-icing aluminum alloy surface with multi-level micro-nano textures constructed by picosecond laser[J]. Materials & design, 2019, 183: 108156.
- [65] FENG L B, YAN Z N, QIANG X H, et al. Facile formation of superhydrophobic aluminum alloy surface and corrosion-resistant behavior[J]. Applied physics A, 2016, 122(3): 165.

- [66] WAN B B, OU J F, LV D M, et al. Superhydrophobic ceria on aluminum and its corrosion resistance[J]. Surface and interface analysis, 2016, 48(3): 173-178.
- [67] XUN X W, WAN Y Z, ZHANG Q C, et al. Low adhesion superhydrophobic AZ31B magnesium alloy surface with corrosion resistant and anti-bioadhesion properties[J]. Applied surface science, 2020, 505: 144566.
- [68] FENG L, ZHANG Y A, XI J M, et al. Petal effect: a superhydrophobic state with high adhesive force[J]. Langmuir, 2008, 24(8): 4114-4119.
- [69] WANG Q, BAI J, DAI B, et al. Robust superhydrophobic diamond microspheres for no-loss transport of corrosive liquid microdroplets[J]. Chemical communications, 2017, 53(15): 2355-2358.
- [70] LI J, YANG Y X, ZHA F, et al. Facile fabrication of superhydrophobic ZnO surfaces from high to low water adhesion[J]. Materials letters, 2012, 75: 71-73.
- [71] LIU Z A, WANG X Y, GAO M Q, et al. Unpowered oil absorption by a wettability sponge based oil skimmer[J]. RSC advances, 2016, 6(91): 88001-88009.
- [72] QIN Z L, XIANG H Q, LIU J G, et al. High-performance oil-water separation polytetrafluoroethylene membranes prepared by picosecond laser direct ablation and drilling [J]. Materials & design, 2019, 184: 108200.
- [73] LIU G Y, WANG J J, WANG W, et al. A novel PET fabric with durable anti-fouling performance for reusable and efficient oil-water separation[J]. Colloids and surfaces A: physicochemical and engineering aspects, 2019, 583: 123941.
- [74] JIN S Y, WANG Y X, MOTLAG M, et al. Large-area direct laser-shock imprinting of a 3D biomimic hierarchical metal surface for triboelectric nanogenerators[J]. Advanced materials, 2018, 30(11): 1705840.
- [75] LIN Z H, CHENG G, LEE S, et al. Harvesting water drop energy by a sequential contact-electrification and electrostatic-induction process[J]. Advanced materials, 2014, 26(27): 4690-4696.
- [76] CHO H D, CHUNG J, SHIN G, et al. Toward sustainable output generation of liquid-solid contact triboelectric nanogenerators: the role of hierarchical structures[J]. Nano energy, 2019, 56: 56-64.
- [77] ZHANG M, CHENG W F, ZHENG Z, et al. Meridian whispering gallery modes sensing in a sessile microdroplet on micro/nanostructured superhydrophobic chip surfaces[J]. Microfluidics and Nanofluidics, 2019, 23(9): 106.
- [78] ACCARDO A, MECARINI F, LEONCINI M, et al. Fast, active droplet interaction: coalescence and reactive mixing controlled by electrowetting on a superhydrophobic surface[J]. Lab on a chip, 2013, 13(3): 332-335.
- [79] DONG S L, WANG Z L, AN L B, et al. Facile fabrication of a superhydrophobic surface with robust micro-/nanoscale hierarchical structures on titanium substrate[J]. Nanomaterials, 2020, 10(8): 1509.
- [80] CHEN Y, LIU J Y, SONG J L, et al. Energy conversion based on superhydrophobic surfaces[J]. Physical chemistry chemical physics, 2020, 22(44): 25430-25444.
- [81] CHEN J, GUO H Y, ZHENG J G, et al. Self-powered triboelectric micro liquid/gas flow sensor for microfluidics[J]. ACS nano, 2016, 10(8): 8104-8112.
- [82] HU S M, SHI Z J, ZHENG R Z, et al. Superhydrophobic liquid-solid contact triboelectric nanogenerator as a droplet sensor for biomedical applications[J]. ACS applied materials & interfaces, 2020, 12(36): 40021-40030.
- [83] WANG G W, GUO Z G. Liquid infused surfaces with anti-icing properties[J]. Nanoscale, 2019, 11(47): 22615-22635.
- [84] CHEN C L, WENG D, MAHMOOD A, et al. Separation mechanism and construction of surfaces with special wettability for oil/water separation[J]. ACS applied materials & interfaces, 2019, 11(11): 11006-11027.
- [85] WANG Z L, WANG A C. On the origin of contact-electrification[J]. Materials today, 2019, 30: 34-51.
- [86] CHEN F F, ZHU Y J, XIONG Z C, et al. Highly flexible superhydrophobic and fire-resistant layered inorganic paper[J]. ACS applied materials & interfaces, 2016, 8(50): 34715-34724.
- [87] WANG S, DU X S, DENG S, et al. A polydopamine-bridged hierarchical design for fabricating flame-retarded, superhydrophobic, and durable cotton fabric[J]. Cellulose, 2019, 26(11): 7009-7023.
- [88] WEN G, GUO Z G. Nonflammable superhydrophobic paper with biomimetic layered structure exhibiting boiling-water resistance and repairable properties for emulsion separation[J]. Journal of materials chemistry A, 2018, 6(16): 7042-7052.
- [89] HUANG X, MUTLU H, THEATO P. A bioinspired hierarchical underwater superoleophobic surface with reversible pH response[J]. Advanced materials interfaces, 2020, 7(8): 2000101.
- [90] SU X J, LI H Q, LAI X J, et al. Stimuli-responsive superhydrophobic films driven by solvent vapor for electric switch and liquid manipulation[J]. Chemical engineering journal, 2020, 394: 124919.
- [91] YANG C, WU L, LI G. Magnetically responsive superhydrophobic surface: in situ reversible switching of water droplet wettability and adhesion for droplet manipulation [J]. ACS applied materials & interfaces, 2018, 10(23): 20150-20158.
- [92] DANIELLO R J, WATERHOUSE N E, ROTHSTEIN J P. Drag reduction in turbulent flows over superhydrophobic surfaces[J]. Physics of fluids, 2009, 21(8): 085103.
- [93] TUO Y J, CHEN W P, F, ZHANG H, et al. One-step hydrothermal method to fabricate drag reduction superhydrophobic surface on aluminum foil[J]. Applied surface science, 2018, 446: 230-235.
- [94] ZHANG S S, OUYANG X, LI J, et al. Underwater drag-reducing effect of superhydrophobic submarine model[J]. Langmuir, 2015, 31(1): 587-593.